National Technical University of Athens
Interdepartmental postgraduate programme in Automated Systems
Control Systems Lab, Mechanical Engineering Department

Dynamics modelling of an umbilical tether for control purposes using Finite Element Method

Author: Dimitrios E. Paraskevas

Supervisor: Professor Kostantinos J. Kyriakopoulos

Athens, 2016

Foreword

This particular diploma thesis is dealing with the dynamics modelling of the umbilical tether that exists in Remotely Operated Vehicles' configuration. This model will be later used for control purposes, so this was a prerequisite during the whole process. The project was implemented in the Control Systems Lab, Mechanical Engineering Department of the National Technical University of Athens, under the supervision of prof. Kostas J. Kyriakopoulos.

I would like to thank prof. Kostas J. Kyriakopoulos for the trust he showed me, his availability and his valuable insight during the whole duration of this project.

Finally, thanks are in order to my parents, for everything they have given and equipped me with so far. I would not be able to achieve anything without their help.

Dimitrios E. Paraskevas

Table of Contents

The only dependable thing about the future is uncertainty

-Amarant Coral-

Introduction

The role of cables in contemporary forms of engineering is fundamental. Cables are used extensively as structural members for many applications, ranging from suspension bridge hangers to kite string. Because of their participation in wide range of applications, cable mechanics has been subject of intensive studies during the last decades.

Within the field of marine technology mooring, crane operations and towing have been the most important applications driving the development of the field forward. Marine cables, towed by ships or submarines, have been used in a variety of civil and military applications. Civilian applications include acoustic surveying for sub-seabed hydrocarbon reservoirs and for the geophysical mapping of ocean basins. Military applications are principally concerned with the detection of submarines. There is also a parallel activity, undertaken for many years now, the laying of undersea communication cables across virtually all of the world's oceans.

On the other hand, in robotics, continuing efforts to establish a more continual presence in the deep ocean are requiring a drastic increase in the number of remotely operated vehicles (ROV) deployments in the ocean floor. Through real time telemetry afforded by the ROV tether, a human operator can control the ROV and the vehicle manipulators, through haptic and visual interfaces. Given the need for a human presence in the control loop, and the lack of any wireless alternative, the tether is a necessity for ROV operation. Thus, it is reasonable to conclude that there is currently a boom in the development of such set-ups from universities, research institutes, third parties and offshore industries.

The problem of predicting the time domain dynamic response of moored and towed cable system is common in many fields of ocean engineering. Understanding the dynamics of these cable systems is crucial for operational and safety concerns. The cable is usually simplified as a flexible tension member and its bending stiffness is neglected because of the extremely large ratio of length over cross section dimension. The motion of the towed cable usually involves large rigid body motion and small elastic stretch.

Nevertheless, often the physics involved in these problems are very complicated and difficult to solve. The marine environment continuously disturbs cable systems through the action of surface water waves, currents, subsurface turbulence, internal water waves and other external disturbances, such as the motions of the supporting vessel and subsystem. These factors cause nonlinear cable geometry plus the dominance of nonlinear hydrodynamic forces, and as a result corresponding equations are highly nonlinear and there can be no analytic solution for that reason. Thus, one needs to turn to numerical approaches in order to solve the problem under consideration.

In practice, what usually interests the engineers and designers is the current position of the cable, and not its displacement. The way the problem is solved, however, can vary widely depending on the application. Modelling methods can be distinguished principally from the way in which they discretize the physical system in space. During this particular diploma thesis pursuit, the methods that have been tackled, and are the main methods which are usually used to model problems of this kind, are listed below:

- Lumped mass cable modeling [1, 2, 3, 4, 6]: This method can be considered as a special case of the general Finite Element method (FEM). It simplifies the coupled nonlinear differential equations of motion into ordinary differential equations by lumping the distributed mass, external loads, inertia forces of the cable to the specified nodes along the cable. The armored cable is discretized into an assembly of N linear elements. The mass is lumped at the $N + 1$ node points, from 0 to N. To model the elasticity of the true cable, each visco-elastic cable element is idealized as a parallel combination of an ideal spring and viscous damper.

- Finite Difference Method [9, 10, 11]: This method was first introduced by Ablow and Schechter [9] in 1983, and was later expanded by Milinazzo et al. [10]. The main differential equations that describe the dynamics of the cable are of the first order in space and time variables. In order to acquire a solution, the main equations need to be discretized, while implementing the necessary boundary conditions, plus the compatibility relations which ensure body continuity during and after deformation has taken place.

The above methods , however, are problem specific and are difficult to be implemented in general purpose analysis programs for complex geometries with multiple cable branches or different cable properties along the length.

- Nodal Position Finite Element Method [14, 15]: In general, the Finite Element Method (FEM) discretizes the cable structure into a finite number of elements. While each element may have different mechanical properties, the equations for each one of them are the same. FEM is simple conceptually, but is valid only for small rotation or increment if the large rigid body rotation is analyzed by an incremental solution. As a result, we chose to implement a novel method that has been successfully used, which solves for the position of an element directly instead of its displacement.

The main focus of this thesis is not only to implement a procedure which predicts the dynamic response of a random cable set-up in water environment, but to also transform the derived equations in such a manner, so as to bring the final system in a control system - like kind of form for future applications.

Thesis structure: In chapters 1 and 2, an overview of Lumped mass and Finite Differences methods is presented, while explicating the pros and cons of each one and the reasons why they were in the end inferior, for the specific scenario in mind at least, to the NPFEM.

In chapter 3, the algorithm actually implemented using the NPFEM is presented. The program used to simulate the phenomena under consideration has been developed using Matlab®, and was created from scratch.

In chapter 4, simulation results are presented, and compared with other papers' results for code validation and method verification.

Finally, in chapter 5, guidelines are given for future research and topics that need to be considered.

Chapter 1
Lumped mass parameter method

As stated earlier above, this method can be considered as a special case of the general Finite Element method (FEM). The method of lumped mass parameter modelling was first introduced by Walton and Polachek [8] in 1960. According to their approach, the cable was considered as a concatenation of inextensible linear elements. The mass of the cable was concentrated, or lumped, at frictionless spherical joints connecting these linear elements. Applying a heuristic procedure, the hydrodynamic, buoyancy and gravitational forces acting over the linear elements were also lumped at the node points. This lumping of the mass and environmental forces allowed the motion of the cable node points to be represented by a series of ordinary differential equations.

The approach that has been studied during this diploma thesis pursuit [1, 2, 6] simplifies the coupled nonlinear differential equations of motion into ordinary differential equations by lumping the distributed mass, external loads, inertia forces of the cable to the specified nodes along the cable. The armored cable is discretized into an assembly of N linear elements. The mass is lumped at the $N+1$ node points, 0 to N. To model the elasticity of the true cable, each visco-elastic cable element is idealized as a parallel combination of an ideal spring and viscous damper.

To aid in the modelling of the cable, we define an inertial reference frame, and a sequence of moving frames attached at points along the cable. A horizontal direction, X, is defined positive to the right, the vertical direction, Z, is defined positive downward, and the Y direction completes the right handed coordinate system. The lumped mass approximation allows for the motion of each node to be calculated independently in the three degrees of freedom, but the elastic internal force of the element constrains the motion of the nodes. The calculation of the elastic tension, damping, and hydrodynamic drag forces is performed in a body-fixed reference frame. Each cable element has a body frame p_1, p_2 and q attached to it, where p_1 is normal, p_2 is binormal and q is tangent to the cable element.

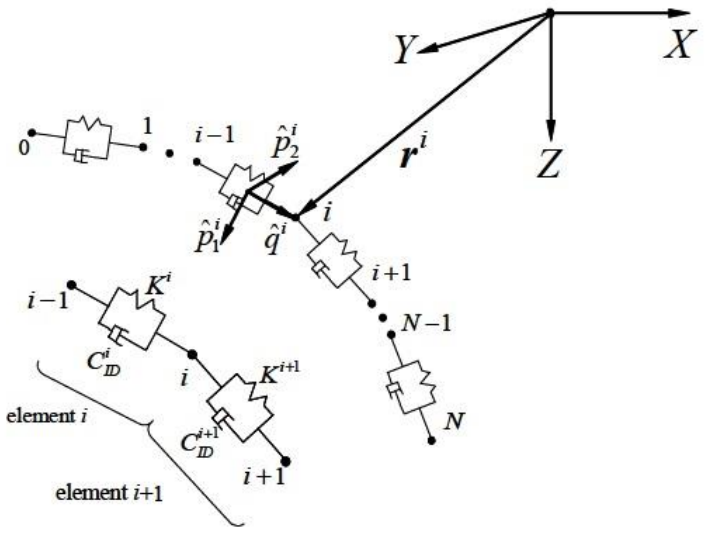

Figure 1. Discrete representation of the marine cable [1]

Kinematics: The orientation of each discretized cable element is represented using a z-y-x $(\psi^i,\ \theta^i,\ \varphi^i)$ Euler angle set. These successive rotations align the inertial frame with the i[th] body frame. If one neglects the torsion of the cable, only two of the three Euler angles are required to specify the orientation of each cable element. Thus, the initial ψ^i rotation is constrained to zero [18]. Applying the specified Euler angle set, the rotation matrix R_{IB}^i that describes the mapping from local to global coordinates (inertial frame) becomes:

$$R_{IB}^i = \begin{bmatrix} \cos\theta^i & \sin\theta^i \sin\varphi^i & \sin\theta^i \sin\varphi^i \\ 0 & \cos\varphi^i & -\sin\varphi^i \\ -\sin\theta^i & \cos\theta^i \sin\varphi^i & \cos\theta^i \cos\varphi^i \end{bmatrix} \quad (1)$$

The Euler angles can be calculated at any instance of the simulation provided that the endpoints of the cable element are known. For example, consider the i[th] element of the cable that is bounded by nodes $i-1$ and i. When expressed in terms of the body fixed frame, the only non-zero component of the vector l^i is in the tangential direction. Thus, it follows that:

$$R_{IB}^i \begin{Bmatrix} 0 \\ 0 \\ l^i \end{Bmatrix} = \begin{Bmatrix} r_X^i - r_X^{i-1} \\ r_Y^i - r_Y^{i-1} \\ r_Z^i - r_Z^{i-1} \end{Bmatrix} \quad (2)$$

, where l^i, the length of the i[th] element at any instant in time is given by:

$$l^i = \sqrt{\left(r_X^i - r_X^{i-1}\right)^2 + \left(r_Y^i - r_Y^{i-1}\right)^2 + \left(r_Z^i - r_Z^{i-1}\right)^2}$$

, and r^i is the position vector, the elements of which describe the location of the i[th] node in the inertial frame. Substitution of (1) into (2), results in the following set of nonlinear equations:

$$\begin{aligned} l^i \sin\theta^i \cos\varphi^i &= r_X^i - r_X^{i-1} \\ -l^i \sin\varphi^i &= r_Y^i - r_Y^{i-1} \\ l^i \cos\theta^i \cos\varphi^i &= r_Z^i - r_Z^{i-1} \end{aligned} \quad (3)$$

Solving the above system of equations yields the following solution for the rotation angles:

$$\theta^i = a\tan 2\left(r_X^i - r_X^{i-1}, r_Y^i - r_Y^{i-1}\right)$$

$$\begin{cases} \varphi^i = \tan^{-1}\left(-\left(r_Y^i - r_Y^{i-1}\right), \dfrac{r_Z^i - r_Z^{i-1}}{\cos\theta^i}\right) \text{ if } \cos\theta^i > \sin\theta^i \\ \varphi^i = \tan^{-1}\left(-\left(r_Y^i - r_Y^{i-1}\right), \dfrac{r_X^i - r_X^{i-1}}{\sin\theta^i}\right) \text{ if } \cos\theta^i < \sin\theta^i \end{cases} \quad (4)$$

Internal forces: By the term internal forces, one refers to the forces that are generated by the elasticity of the cable elements, which results in the stretch of the elements in the tangent direction.

According to [4], the tension within the i[th] cable element T^i acts in the tangential direction and is modeled as a linear function of the tangential strain of the element ε^i:

$$T^i = EA\varepsilon^i$$
$$\varepsilon^i = \frac{L^i - L_u^i}{L_u^i} \quad (5)$$

, where:

- L_u^i is the unstretched length of the corresponding cable element
- A is the cross sectional area of the element
- E is the effective Young's modulus of the cable

It has been observed that during cable motion, the friction between the braids of the cable will dissipate energy within the cable structure. Obviously, this calls for some form of damping modeling. This phenomenon is modeled as a linear viscous damping effect, with axial force being generated defined as follows:

$$P^i = C_{ID}\varepsilon^i$$
$$\varepsilon^i = \frac{v_{q^i}^{(i)} - v_{q^i}^{(i-1)}}{L_u^i} \quad (6)$$

, where:

- C_{ID} is the internal viscous damping coefficient of the cable structure
- $v_{q^i}^{(i)}$ is the component of the i[th] node velocity $v^{(i)} = \left\{ v_{p_1^i}^{(i)} \quad v_{p_2^i}^{(i)} \quad v_{q^i}^{(i)} \right\}^T$ in the tangential direction

External forces: The external forces are a result of the cable structure's interaction with the surrounding environment. They mainly consist of hydrodynamic drag, weight and buoyancy effects. One has also to consider applied loads, namely forces that can be defined explicitly in terms of time.

The drag forces can be calculated as follows:

$$h_{p_1^i}^i = -\frac{1}{2}\rho_w C_D d_c L_u^i f_p \left|v^i\right|^2 \frac{v_{p_1^i}^i}{\sqrt{\left(v_{p_1^i}^i\right)^2 + \left(v_{p_2^i}^i\right)^2}}$$
$$h_{p_2^i}^i = -\frac{1}{2}\rho_w C_D d_c L_u^i f_p \left|v^i\right|^2 \frac{v_{p_2^i}^i}{\sqrt{\left(v_{p_1^i}^i\right)^2 + \left(v_{p_2^i}^i\right)^2}} \quad (7)$$
$$h_{p_1^i}^i = -\mathrm{sgn}\left(v_{q^i}^i\right)\rho_w C_D d_c L_u^i f_q \left|v^i\right|^2$$

, where:

- $h_{p_1}^i, h_{p_2}^i, h_q^i$ are the hydrodynamic drag components in terms of body fixed representation
- ρ_w is the density of the water
- d_c is the cable diameter
- C_D is the normal drag coefficient of the cable
- v^i is the velocity of the geometric center of the element, with respect to the surrounding fluid
- f_p, f_q are loading functions which modify the drag coefficient, that depend on the incidence angle of the relative fluid flow

The mass and buoyancy of the i[th] cable element are given by:

$$m_c^i = \rho_c V_c^i$$
$$b^i = \rho_w g V_c^i .$$

, where:

- ρ_c is the density of the cable
- $g = \{0 \quad 0 \quad g\}^T$ is the gravity acceleration, in terms of the inertial frame
- b^i buoyancy force of the cable element expressed in the inertial frame
- V_c^i is the volume of the corresponding cable element

Finally, the effects of added mass are accounted for in the calculation of the cable element mass matrix. Using the assumption that there are no added mass effects in the tangential direction, one can write the element mass matrix as follows:

$$M_B^i = \begin{bmatrix} m_c^i + m_a^i & 0 & 0 \\ 0 & m_c^i + m_a^i & 0 \\ 0 & 0 & m_c^i \end{bmatrix} \quad (8)$$

In order to be used in the governing equations of motion, the mass matrix needs to be transformed using the rotation matrix R_{IB}^i. The mass attributed to the i^{th} node is formed from contributions of elements above and below the node. Thus:

$$M_I^i = \frac{1}{2} R_{IB}^i M_B^i \left(R_{IB}^i\right)^T + \frac{1}{2} R_{IB}^{i+1} M_B^{i+1} \left(R_{IB}^{i+1}\right)^T \quad (9)$$

Assembly of forces: Application of Newton's second law to the nodes of the lumped mass representation yields asset of $3(N+1)$ second order differential equations (where N is the number of the elements in which the cable is discretized into), which govern the motion of the nodes in the X, Y, Z directions. Thus, the equation of translational motion of the i^{th} node of the tether $(0 \le i \le N)$ becomes:

$$M_I^i \ddot{r}^{(i)} = R_{IB}^{i+1}\left[\left(t^{i+1} + p^{i+1}\right) + \frac{1}{2}h^{i+1}\right] - R_{IB}^{i}\left[\left(t^{i} + p^{i}\right) - \frac{1}{2}h^{i}\right] + \frac{1}{2}\left(m_c^i g + b^i + m_c^{i+1} g + b^{i+1}\right) + f_a^i \quad (10)$$

In order to solve the above equation, the author proposes a transformation of (10) into a system of $6(N+1)$ first order differential equations to afford the use of a 4th order Runge-Kutta approach, with the appropriate boundary conditions (either kinematic or dynamic) at nodes 0 and N specified accordingly. Assuming a time dependent state vector of the following form:

$$Y(t) = \left\{ r^{(0)}(t) \quad \dot{r}^{(0)}(t) \quad r^{(1)}(t) \quad \cdots \quad \dot{r}^{(N-1)}(t) \quad r^{(N)}(t) \quad \dot{r}^{(N)}(t) \right\}^T$$

Given an initial state of the tether, one can augment the node acceleration with the velocities of the current tether state to form the first time differential of the state vector $\dot{Y}(t_k)$. This vector is then passed to the chosen integration scheme in order to produce $Y(t_{k+1})$.

The method presented and its' solution procedure described [1] is pretty much straightforward and easily understood conceptually. However, the above mentioned control transformation proved to be harder than expected, with no guarantee that it could be effectively used for the desired control purposes later on. That was mostly due to the high nonlinearity nature and the non-systematic representation of the loads equations. This rendered variable separation and consequent transformation of the problem into a meaningful control form a burdensome task.

Chapter 2
Finite differences method

This method was first introduced by Ablow and Schechter [9], and was some years later expanded by Milinazzo et al., who introduced a number of modifications in order to produce a more efficient and stable method of computing, applied in towed cable systems [10]. The main differential equations that describe the dynamics of the cable are of the first order in space (s) and time (t) variables. In order to acquire a solution, the main equations need to be discretized.

Kinematics: During the modelling procedure, the cable is treated as a single curvilinear line. Let s denote the unstretched Lagrangian coordinate along the cable, measured from the origin of the coordinate system to a material point on the cable. Usually, the origin is chosen so as to coincide with a boundary, and is denoted as $s = 0$. The other endpoint is denoted as $s = L$.

The cable is taken to be extensible, so we define $p(t, s)$ as the stretched distance to the same material point s, at time t. The longitudinal strain e is defined as follows:

$$e = \lim_{\delta s \to 0} \frac{\delta p - \delta s}{\delta s} = \frac{dp}{ds} - 1 \qquad (11)$$

The cable cross sectional area is also altered due to elongation. Assuming that the cable has a Poisson's ratio of $\frac{1}{2}$ means that its' volume is preserved after stretching. The change in cable diameter d for the typical case of a cross-sectional area is:

$$d = d_s \left(1 + e\right)^{\frac{1}{2}}$$

The coordinate system is resolved into the tangent, normal and binormal directions, given by the unit vectors $\hat{t},\ \hat{n},\ \hat{b}$ respectively. The tangential direction is defined as tangent to the cable, pointing in the direction of increasing s. The normal direction is perpendicular to $\hat{t}$ and the binormal direction is defined in such a way the resulting system is orthogonal and right-handed.

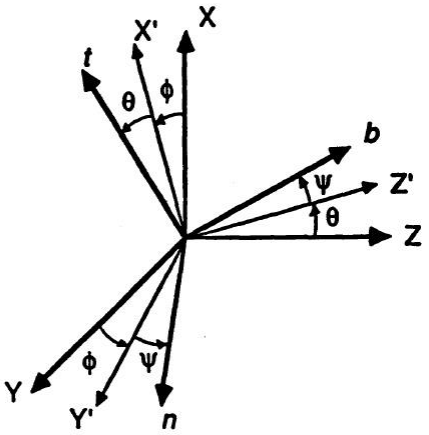

Figure 2. Coordinate system and Euler rotation sequence [11]

The transformation between the Lagrangian coordinates x, y, z and the fixed coordinates X, Y, Z is accomplished through a set of rotations (Euler angles).

$$\begin{bmatrix} x \\ y \\ z \end{bmatrix} = \Gamma \begin{bmatrix} X \\ Y \\ Z \end{bmatrix} \tag{12}$$

The balance of forces at a point of a cable may be written as follows:

$$\frac{\partial}{\partial S} T + W + F + B = 0 \tag{13}$$

, where:

- S is the distance along the stretched cable
- T is the tension
- W is the weight minus buoyancy per unit length
- F is the force exerted on the cable by the fluid per unit length
- B is the d'Alembert force of the cable motion per unit length

The cable is assumed to be elastic, thus extensible, and to have a circular cross section area. Without loss of generality, consider the 2d cable dynamics problem. The governing equations of motion are as following:

$$\begin{aligned}
&T'(\varepsilon)\frac{\partial \varepsilon}{\partial s} - S_n \frac{\partial \varphi}{\partial s} - m\frac{\partial u}{\partial t} + mv\frac{\partial \varphi}{\partial t} - w_0 \cos\varphi - \frac{1}{2}\rho_w d C_{D_t} u_r |u_r| \sqrt{1+\varepsilon} = 0 \\
&\left\{ \begin{aligned} &\frac{\partial S_n}{\partial s} + T\varepsilon\frac{\partial \varphi}{\partial s} - (m+m_a)\frac{\partial v}{\partial t} - \left[mu + \left(\rho_w \frac{\pi d^2}{4} + m_a \right)(U\cos\varphi + V\sin\varphi) \right] \frac{\partial \varphi}{\partial t} \\ &+ w_0 \sin\varphi - \frac{1}{2}\rho_w d C_{D_n} v_r |v_r| \sqrt{1+\varepsilon} = 0 \end{aligned} \right\} \\
&\frac{\partial u}{\partial s} - v\frac{\partial \varphi}{\partial s} - \frac{\partial \varepsilon}{\partial t} = 0 \\
&\frac{\partial v}{\partial s} + u\frac{\partial \varphi}{\partial s} - (1+\varepsilon)\frac{\partial \varphi}{\partial t} = 0 \\
&\frac{\partial \varphi}{\partial s} - \Omega_3 = 0 \\
&EI\frac{\partial \Omega_3}{\partial s} + S_n (1+\varepsilon)^3 = 0
\end{aligned} \tag{14}$$

, where the cable properties are defined by:

- $T(\varepsilon)$ is the tension strain relationship
- w_0 is the wet weight of the cable
- $m,\ m_a$ are the mass and added mass per unit length of the structure, respectively
- d is the diameter of the cable
- $C_{d_n},\ C_{d_t}$ are the normal and tangential drag coefficients

The motion and force state of the cable are completely described by the following 6 d.o.f:

- tangential and normal velocities, u and v
- strain ε
- shear force S_n
- Inclination φ
- and the curvature of the cable Ω_3, which is introduced to remove higher order derivatives of φ

Finally, the sea current is given in the global vertical and horizontal coordinates by U and V respectively. In this case, u_r and v_r represent the relative velocities in local coordinates, which are defined as follows:

$$\begin{aligned} u_r &= u - U\cos\varphi - V\sin\varphi \\ v_r &= v + U\sin\varphi - V\cos\varphi \end{aligned} \tag{15}$$

If one wishes to write the problem in matrix form:

$$M\frac{\partial Y}{\partial t} + K\frac{\partial Y}{\partial s} + F = 0 \tag{16}$$

, the matrices have to be defined as follows:

$$Y = \left[\varepsilon, S_n, u, v, \varphi, \Omega_3\right]^T \tag{16a}$$

$$M = \begin{bmatrix} 0 & 0 & -m & 0 & mv & 0 \\ 0 & 0 & 0 & -(m+m_a) & 0 & 0 \\ -1 & 0 & 0 & 0 & 0 & 0 \\ 0 & 0 & 0 & 0 & -(1+\varepsilon) & 0 \\ 0 & 0 & 0 & 0 & 0 & 0 \\ 0 & 0 & 0 & 0 & 0 & 0 \end{bmatrix}$$

$$K=\begin{bmatrix} T'(\varepsilon) & 0 & 0 & 0 & -S_n & 0 \\ 0 & 1 & 0 & 0 & T(\varepsilon) & 0 \\ 0 & 0 & 1 & 0 & -v & 0 \\ 0 & 0 & 0 & 1 & u & 0 \\ 0 & 0 & 0 & 0 & 1 & 0 \\ 0 & 0 & 0 & 0 & 0 & EI \end{bmatrix}$$

$$F=\begin{bmatrix} -w_0\cos\varphi-\frac{1}{2}\rho_w dC_{D_t}u_r|u_r|\sqrt{1+\varepsilon} \\ w_0\sin\varphi-\frac{1}{2}\rho_w dC_{D_n}v_r|v_r|\sqrt{1+\varepsilon} \\ 0 \\ 0 \\ -\Omega_3 \\ S_n(1+\varepsilon)^3 \end{bmatrix} \qquad (16b)$$

Vector Y essentially contains the problem's state variables.

The discretization of the governing's partial differential equation can procced in several ways. A straightforward method is to use finite differences in both time and space using the box method. The discretization is applied on the half grid points. As a result, the method is supposed to be second order accurate. During our avocation with it, this has been mathematically proven to be true (see appendix for more information on the subject).

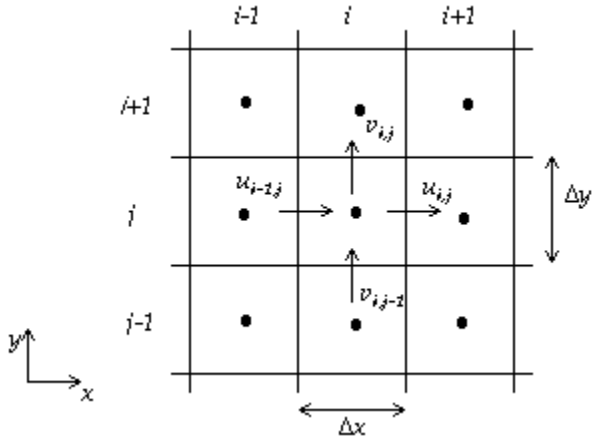

Figure 3. Stencil of the box discretization method

As was stated earlier, in our case, we need to cast the problem in some kind of form that resembles the classical control form structure, implying $\dot{x} = A(t)x(t) + B(t)u(t)$. In order to do this, the first step is to apply the spatial discretization at half grid points. This will result in the vanishing of the space variable from the partial differential governing equation, thus transforming it in a differential equation with respect to time only. Application of spatial discretization at each half grid point yields:

$$M_{j-0.5}\begin{bmatrix}\dot{Y}_{j-1}\\ \dot{Y}_{j}\end{bmatrix} + K_{j-0.5}\begin{bmatrix}Y_{j-1}\\ Y_{j}\end{bmatrix} + F_{j-0.5} = 0 \qquad (17)$$

, with the matrices presented above being defined as:

$$M_{j-0.5} = \begin{bmatrix} 0 & 0 & -m_{j-1} & 0 & (mv)_{j-1} & 0 \\ 0 & 0 & 0 & -(m+m_a)_{j-1} & -\left[mu+\left(\rho\frac{\pi d^2}{4}+m_a\right)(U\cos\varphi+V\sin\varphi)\right]_{j-1} & 0 \\ -1 & 0 & 0 & 0 & 0 & 0\cdots \\ 0 & 0 & 0 & 0 & -(1+\varepsilon)_{j-1} & 0 \\ 0 & 0 & 0 & 0 & 0 & 0 \\ 0 & 0 & 0 & 0 & 0 & 0 \end{bmatrix}$$

$$\begin{bmatrix} 0 & 0 & -m_{j} & 0 & (mv)_{j} & 0 \\ 0 & 0 & 0 & -(m+m_a)_{j} & -\left[mu+\left(\rho\frac{\pi d^2}{4}+m_a\right)(U\cos\varphi+V\sin\varphi)\right]_{j} & 0 \\ \cdots -1 & 0 & 0 & 0 & 0 & 0 \\ 0 & 0 & 0 & 0 & -(1+\varepsilon)_{j} & 0 \\ 0 & 0 & 0 & 0 & 0 & 0 \\ 0 & 0 & 0 & 0 & 0 & 0 \end{bmatrix} \qquad (17a)$$

$$K_{j-0.5}=\begin{bmatrix} -\left(T_j^{'}+T_{j-1}^{'}\right) & 0 & 0 & 0 & \left(S_{n_j}+S_{n_{j-1}}\right) & 0 \\ 0 & -2 & 0 & 0 & -\left(T_j+T_{j-1}\right) & 0 \\ 0 & 0 & -2 & 0 & v_j+v_{j-1} & 0 \\ 0 & 0 & 0 & -2 & -\left(u_j+u_{j-1}\right) & 0 \\ 0 & 0 & 0 & 0 & -2 & 0 \\ 0 & 0 & 0 & 0 & 0 & -2EI \end{bmatrix} \ldots$$

$$\ldots \begin{bmatrix} \left(T_j^{'}+T_{j-1}^{'}\right) & 0 & 0 & 0 & -\left(S_{n_j}+S_{n_{j-1}}\right) & 0 \\ 0 & 2 & 0 & 0 & \left(T_j+T_{j-1}\right) & 0 \\ 0 & 0 & 2 & 0 & -\left(v_j+v_{j-1}\right) & 0 \\ 0 & 0 & 0 & 2 & \left(u_j+u_{j-1}\right) & 0 \\ 0 & 0 & 0 & 0 & 2 & 0 \\ 0 & 0 & 0 & 0 & 0 & 2EI \end{bmatrix} \quad (17b)$$

$$F_{j-0.5}=\begin{bmatrix} -w_0\left(\cos\varphi_j+\cos\varphi_{j-1}\right)-\frac{1}{2}\rho_w dC_{D_t}\left[\left(u_r\left|u_r\right|\sqrt{1+\varepsilon}\right)_j+\left(u_r\left|u_r\right|\sqrt{1+\varepsilon}\right)_{j-1}\right] \\ w_0\left(\sin\varphi_j+\sin\varphi_{j-1}\right)-\frac{1}{2}\rho_w dC_{D_t}\left[\left(v_r\left|v_r\right|\sqrt{1+\varepsilon}\right)_j+\left(v_r\left|v_r\right|\sqrt{1+\varepsilon}\right)_{j-1}\right] \\ 0 \\ 0 \\ -\left(\Omega_{3_j}+\Omega_{3_{j-1}}\right) \\ \left[S_n\left(1+\varepsilon\right)^3\right]_j+\left[S_n\left(1+\varepsilon\right)^3\right]_{j-1} \end{bmatrix} \quad (17c)$$

Writing the equations for all nodes, one gets:

$$\left.\begin{aligned} &M_{0.5}\begin{bmatrix}\dot{Y}_0\\ \dot{Y}_1\end{bmatrix}+K_{0.5}\begin{bmatrix}Y_0\\ Y_1\end{bmatrix}+F_{0.5}=0 \\ &M_{1.5}\begin{bmatrix}\dot{Y}_1\\ \dot{Y}_2\end{bmatrix}+K_{1.5}\begin{bmatrix}Y_1\\ Y_2\end{bmatrix}+F_{1.5}=0 \\ &M_{2.5}\begin{bmatrix}\dot{Y}_2\\ \dot{Y}_3\end{bmatrix}+K_{2.5}\begin{bmatrix}Y_2\\ Y_3\end{bmatrix}+F_{2.5}=0 \\ &\vdots \\ &M_{N-0.5}\begin{bmatrix}\dot{Y}_{N-1}\\ \dot{Y}_N\end{bmatrix}+K_{N-0.5}\begin{bmatrix}Y_{N-1}\\ Y_N\end{bmatrix}+F_{N-0.5}=0 \end{aligned}\right\} \text{n instances, where n = N-1 (N nodes)}$$

Assembling the blocks associated with all nodes, we derive a form of global equation, as follows:

$$M_G\dot{Y} + K_G Y + F_G = 0$$

$$M_G = \begin{bmatrix} (A_0)_{3x6} & 0 & 0 & 0 & 0 & 0 \\ (M_{0.5})_{6x12} & 0 & 0 & 0 & 0 & 0 \\ 0 & (M_{1.5})_{6x12} & 0 & 0 & 0 & 0 \\ \ddots & \ddots & \ddots & \ddots & \ddots & \ddots \\ 0 & 0 & 0 & 0 & (M_{N-0.5})_{6x12} & 0 \\ 0 & 0 & 0 & 0 & 0 & (A_N)_{3x6} \end{bmatrix} \quad (18a)$$

$$K_G = \begin{bmatrix} (B_0)_{3x6} & 0 & 0 & 0 & 0 & 0 \\ (K_{0.5})_{6x12} & 0 & 0 & 0 & 0 & 0 \\ 0 & (K_{1.5})_{6x12} & 0 & 0 & 0 & 0 \\ \ddots & \ddots & \ddots & \ddots & \ddots & \ddots \\ 0 & 0 & 0 & 0 & (K_{N-0.5})_{6x12} & 0 \\ 0 & 0 & 0 & 0 & 0 & (B_N)_{3x6} \end{bmatrix}$$

$$F_G = \begin{bmatrix} \text{node \#0 boundaries } (3 \text{ equations}) \\ F_{0.5} \\ F_{1.5} \\ \vdots \\ F_{N-0.5} \\ \text{node \#N boundaries } (3 \text{ equations}) \end{bmatrix} \quad (18b)$$

Since we are going to investigate the dynamics from a control perspective, at some point in the process, matrix M_G will have to be inverted. This means that one has to make sure that M^{-1} exists. Unfortunately, typical boundary conditions are described in terms of state variables, not their derivatives (usually being kinematic constraints or known forces at both ends). This means that typically $A_0 = A_N = 0_{3x6}$, which obviously renders matrix M_G non-invertible.

Appendix

Box method accuracy: In order to verify the stability and the accuracy of the proposed method, it is common practice to consider the application of the method to the corresponding single degree of freedom, linear, homogenous problem:

$$\frac{\partial y}{\partial t}+\omega\frac{\partial y}{\partial s}=0 \tag{19}$$

Applying the box discretization technique, one derives the following equation:

$$\frac{1}{2}\left[\frac{y_j^n-y_j^{n-1}}{\Delta t}+\frac{y_{j-1}^n-y_{j-1}^{n-1}}{\Delta t}\right]+\frac{1}{2}\omega\left[\frac{y_j^n-y_{j-1}^n}{\Delta s}+\frac{y_j^{n-1}-y_{j-1}^{n-1}}{\Delta s}\right]=0 \tag{18}$$

Assume that $\tilde{y}$ is an exact solution to the continuous differential equation. Using Taylor series expansion for $s=j\Delta s, t=n\Delta t$ around the defined solution above, yields:

$$\begin{aligned}
\tilde{y}_j^{n-1} &= \tilde{y}_j^n-\Delta t\left(\frac{\partial\tilde{y}}{\partial t}\right)_j^n+\frac{\Delta t^2}{2}\left(\frac{\partial^2\tilde{y}}{\partial t^2}\right)_j^n-\frac{\Delta t^3}{6}\left(\frac{\partial^3\tilde{y}}{\partial t^3}\right)_j^n+\dots\\
\tilde{y}_{j-1}^n &= \tilde{y}_j^n-\Delta s\left(\frac{\partial\tilde{y}}{\partial s}\right)_j^n+\frac{\Delta s^2}{2}\left(\frac{\partial^2\tilde{y}}{\partial s^2}\right)_j^n-\frac{\Delta s^3}{6}\left(\frac{\partial^3\tilde{y}}{\partial s^3}\right)_j^n+\dots\\
\tilde{y}_{j-1}^{n-1} &= \tilde{y}_j^n-\Delta t\left(\frac{\partial\tilde{y}}{\partial t}\right)_j^n-\Delta s\left(\frac{\partial\tilde{y}}{\partial s}\right)_j^n\\
&\quad+\frac{\Delta t^2}{2}\left(\frac{\partial^2\tilde{y}}{\partial t^2}\right)_j^n+\frac{\Delta s^2}{2}\left(\frac{\partial^2\tilde{y}}{\partial s^2}\right)_j^n+\Delta s\Delta t\left(\frac{\partial^2\tilde{y}}{\partial s\partial t}\right)_j^n\\
&\quad-\frac{\Delta t^3}{6}\left(\frac{\partial^3\tilde{y}}{\partial t^3}\right)_j^n-\frac{\Delta s^3}{6}\left(\frac{\partial^3\tilde{y}}{\partial s^3}\right)_j^n-\frac{\Delta t\Delta s^2}{2}\left(\frac{\partial^3\tilde{y}}{\partial t\partial s^2}\right)_j^n-\frac{\Delta t^2}{2}\left(\frac{\partial^3\tilde{y}}{\partial t^2\partial s}\right)_j^n+\dots
\end{aligned} \tag{21}$$

Since $\tilde{y}$ is an exact solution to the problem, one can write:

$$\left(\frac{\partial \tilde{y}}{\partial t}\right)_j^n = -\omega\left(\frac{\partial \tilde{y}}{\partial s}\right)_j^n$$
$$\left(\frac{\partial^2 \tilde{y}}{\partial t^2}\right)_j^n = -\omega\left(\frac{\partial^2 \tilde{y}}{\partial s \partial t}\right)_j^n$$
$$\left(\frac{\partial^2 \tilde{y}}{\partial s \partial t}\right)_j^n = -\omega\left(\frac{\partial^2 \tilde{y}}{\partial s^2}\right)_j^n \qquad (22)$$
$$\left(\frac{\partial^3 \tilde{y}}{\partial s \partial t^2}\right)_j^n = -\omega\left(\frac{\partial^3 \tilde{y}}{\partial s^2 \partial t}\right)_j^n, \text{ etc } \ldots$$

Substituting (21) and (22) into (20) yields:

$$\frac{1}{2}\left[\frac{y_j^n - y_j^{n-1}}{\Delta t} + \frac{y_{j-1}^n - y_{j-1}^{n-1}}{\Delta t}\right] + \frac{1}{2}\omega\left[\frac{y_j^n - y_{j-1}^n}{\Delta s} + \frac{y_j^{n-1} - y_{j-1}^{n-1}}{\Delta s}\right] =$$
$$\Delta t^2\left[\frac{1}{6}\left(\frac{\partial^3 \tilde{y}}{\partial t^3}\right)_j^n + \frac{\omega}{4}\left(\frac{\partial^3 \tilde{y}}{\partial s \partial t^2}\right)_j^n\right] + \Delta s^2\left[\frac{1}{4}\left(\frac{\partial^3 \tilde{y}}{\partial s^2 \partial t}\right)_j^n + \frac{\omega}{6}\left(\frac{\partial^3 \tilde{y}}{\partial s^3}\right)_j^n\right] + H.O.T \qquad (23)$$

Chapter 3
Nodal Position Finite Element Method

The following is based on [15, 16] that describe a new nodal position finite element method (FEM) for use in the simulation of the dynamics of towed body systems. The method assumes superiority to conventional FEM methods, in the sense that it solves the problem for the position of the cable directly and not indirectly via the displacements.

Consider a two-node straight cable element in 3-d space. Element geometry is described by its nodal coordinates (X_i, Y_i, Z_i) $(i = 1,2)$ in the global coordinate system. Define X_e such that

$$X_e = \left[X_1, Y_1, Z_1, X_2, Y_2, Z_2\right]^T \quad (24)$$

If one wishes to express the position and its time derivatives in terms of the element shape functions and nodal values, then one has:

$$\begin{aligned} R &= NX_e \\ v &= \dot{R} = N\dot{X}_e \\ a &= \ddot{R} = N\ddot{X}_e \end{aligned} \quad (25)$$

, where:

- $R = \{\mathrm{X}, \mathrm{Y}, \mathrm{Z}\}^{\mathrm{T}}$ is the global position of the arbitrary point
- $v = \{v_x, v_y, v_z\}^T$ and $a = \{a_x a_y a_z\}^T$ are the velocity and acceleration vectors of the arbitrary point, and N is the element shape functions, such that:

$$\begin{aligned} N &= \left[I_{3x3}\left(1-\xi\right) \quad I_{3x3}\,\xi\right] \\ \xi &= x / L \\ L &= \sqrt{\left(X_2^2 - X_1^2\right) + \left(Y_2^2 - Y_1^2\right) + \left(Z_2^2 - Z_1^2\right)} \end{aligned} \quad (26)$$

The Green - Lagrangian strain of the element is defined as:

$$\varepsilon_x = \frac{L}{L_0} - 1 = BX_e - 1 \quad (27)$$

, where B is the strain matrix, defined as:

$$B = \begin{bmatrix} -\frac{\cos\theta_x}{L_0} & -\frac{\cos\theta_y}{L_0} & -\frac{\cos\theta_z}{L_0} & \frac{\cos\theta_x}{L_0} & \frac{\cos\theta_y}{L_0} & \frac{\cos\theta_z}{L_0} \end{bmatrix}$$
$$= \begin{bmatrix} \frac{X_1 - X_2}{LL_0} & \frac{Y_1 - Y_2}{LL_0} & \frac{Z_1 - Z_2}{LL_0} & -\frac{X_1 - X_2}{LL_0} & -\frac{Y_1 - Y_2}{LL_0} & -\frac{Z_1 - Z_2}{LL_0} \end{bmatrix} \quad (28)$$

Mass matrix

The mass matrix is derived from the kinetic energy of the element, as follows:

$$T = \frac{1}{2}\int_0^L \rho A \dot{R}\dot{R} dx = \frac{1}{2}\dot{X}_e^T M \dot{X}_e$$
$$M = \frac{\rho AL}{6}\begin{bmatrix} 2I_{3x3} & I_{3x3} \\ I_{3x3} & 2I_{3x3} \end{bmatrix} \quad (29)$$

, where ρ, A are the material density and the cross sectional area respectively. The element mass matrix is expressed in the global coordinate system and as it is apparent, is constant.

Stiffness matrix

The stiffness matrix can be derived from the strain energy of the element, as follows:

$$U = \frac{1}{2}\int_0^L EA\varepsilon_x^2 dx = \frac{1}{2}X_e^T K X_e - X_e^T F_k \frac{1}{2}EAL$$
$$K = \frac{EAL}{L_0^2}\begin{bmatrix} Q & -Q \\ -Q & Q \end{bmatrix}$$
$$F_k = EALB^T \quad (30)$$
$$Q = \begin{bmatrix} \cos^2\theta_x & \cos\theta_x\cos\theta_y & \cos\theta_x\cos\theta_z \\ \cos\theta_y\cos\theta_x & \cos^2\theta_y & \cos\theta_y\cos\theta_z \\ \cos\theta_z\cos\theta_x & \cos\theta_z\cos\theta_y & \cos^2\theta_z \end{bmatrix}$$

, where:

- E is the Young's modulus of the cable element
- K is the stiffness matrix of the element
- F_k is the generalized nodal force vector resulting from the elasticity of the cable element

Like the mass matrix, the stiffness matrix is also expressed in the global coordinate system. It is highly nonlinear and decoupling into linear and nonlinear part cannot be achieved as in the conventional FEM method.

Material viscous damping matrix

Since a system without damping is virtually non-existent, the author of the method under consideration introduces a damping matrix of the following form:

$$C = \beta\left[M + M_a\right] + \gamma K \quad (31)$$

, where:

- β, γ are the Rayleigh damping coefficients
- M_a is the added mass matrix (see below)

In order to calculate the Rayleigh damping coefficients, one can employ many formulas. In our case, we chose to approximate them by employing the calculation of the natural frequencies of the system. The relationship between multiple experimental modal analysis frequency and damping estimates and the coefficients (α and β) can be derived using the frequency domain version of the equations (see appendix for more information on the subject).

Fluid dynamic force vectors (Drag + added mass effects)

Drag effects can be modelled as follows:

$$\begin{aligned} f_{dn} &= -C_{dn}(\alpha)\frac{\rho_0 D}{2}V^2\frac{V_n}{|V_n|} \\ f_{dt} &= -C_{dt}(\alpha)\frac{\rho_0 D}{2}V^2\frac{V_t}{|V_t|} \\ f_a &= -C_m\rho_0 A\dot{V}_n \\ V &= \dot{R} - V_e \\ V_n &= (I - k_0)V \\ V_t &= k_0 V \end{aligned} \quad (32)$$

, where:

- $f_{dn}, f_{dt}, C_{dn}, C_{dt}$ are the drag components normal and tangent to the element and their respective loading functions
- a is the angle of attack, and f_a is the inertial force normal to the element resulting from the added mass of fluid surrounding the element
- Finally, V_c is the free stream velocity of the fluid (see appendix for more information on the subject)

Virtual work done by the inertial force of the added mass effect is:

$$\delta W_a = \int_0^L f_a \delta R dx = -\delta X_e^T M_a \ddot{X}_e + \delta X_e^T F_a$$
$$M_a = \frac{C_m \rho_0 AL}{6}\left(M_{a0} - M_{a1}\right) = \frac{C_m \rho_0 AL}{6}\begin{bmatrix} 2\left(I_{3x3} - Q\right) & I_{3x3} - Q \\ I_{3x3} - Q & 2\left(I_{3x3} - Q\right) \end{bmatrix} \quad (33)$$
$$F_a = M_a \dot{V}_c^e$$

, where $\dot{V}_c^e$ is the fluid acceleration vector at the element nodes.

The drag forces will be calculated in the local element coordinates. The local coordinate system is assumed to be constructed in the following way (see appendix for more information on the subject):

The x axis is aligned with the cable element, the y axis is aligned with the plane containing the x axis and the relative fluid velocity but normal to the element, and the z axis is the cross product of x and y. Thus, the fluid velocity relative to the element in the local coordinates can be written as:

$$v = \dot{r} - v_c = \begin{bmatrix} \dot{x} - v_{cx} & \dot{y} - v_{cy} & 0 \end{bmatrix}^T \quad (34)$$

It follows that the drag force vector can be expressed in the local coordinates, as follows:

$$f_d = \frac{\rho_0 D}{2} v^2 \begin{bmatrix} -C_{dt}(\alpha)\, sign(v_x) & -C_{dn}(\alpha)\, sign(v_y) & 0 \end{bmatrix}^T \quad (35)$$

The virtual work done by the drag forces is given by:

$$\delta W_d = \int_0^L f_d \delta r dx = -\delta x_e^T f_d^e$$
$$f_d^e = \begin{bmatrix} C_{dt}(a)\frac{\rho_0 D}{2} sign(v_x) f_1 \\ C_{dn}(a)\frac{\rho_0 D}{2} sign(v_y) f_1 \\ 0 \\ C_{dt}(a)\frac{\rho_0 D}{2} sign(v_x) f_2 \\ C_{dn}(a)\frac{\rho_0 D}{2} sign(v_y) f_2 \\ 0 \end{bmatrix} \quad (36)$$

$$f_i = \dot{x}_e^T A_i \dot{x}_e - 2\dot{x}_e^T A_i v_e + v_e^T A_i v_e$$
$$A_1 = \frac{1}{12}\begin{bmatrix} 3I_{3x3} & I_{3x3} \\ I_{3x3} & I_{3x3} \end{bmatrix} \quad (36a)$$
$$A_2 = \frac{1}{12}\begin{bmatrix} I_{3x3} & I_{3x3} \\ I_{3x3} & 3I_{3x3} \end{bmatrix}$$

, where f_d^e is the equivalent nodal drag forces vector expressed in the local coordinates. Since we are going to write the equations of motion in the global coordinate system, one has to transform the drag forces from local to global coordinates using the standard FEM coordinate transformation matrix.

$$F_d = T^T f_d^e \quad (37)$$

Buoyant and gravity forces

Gravitational forces in global coordinates are given such as:

$$f_{bg} = \begin{bmatrix} 0 & 0 & -A(\rho - \rho_0)g \end{bmatrix}^T \quad (38)$$

, where g is the acceleration due to gravity. Accordingly, the virtual work done by the gravitational forces is given by:

$$\delta W_{bg} = \int_0^L A\rho_0 N^T f_b dx = \delta X_e^T F_{bg}$$
$$F_{bg} = -\frac{LA(\rho - \rho_0)g}{2}\begin{bmatrix} 0 \\ 0 \\ 1 \\ 0 \\ 0 \\ 1 \end{bmatrix} \quad (39)$$

, where F_{bg} is the equivalent nodal buoyant force vector.

Equations of motion

The equations of motion of a single element, derived from the principle of virtual work, are as follows:

$$\begin{aligned} &\delta U - \delta T - \delta W_v - \delta W_a - \delta W_d - \delta W_{bg} = 0 \Rightarrow \\ &\left[M + M_a\right]\ddot{X}_e + C\dot{X}_e + KX_e = F_k + F_a + F_{bg} - F_d \end{aligned} \quad (40)$$

The equations derived describe the dynamics of a single element for the problem without exogenous input. If the configuration dictates a force input to the system, then one has to simply add the applied loads to the corresponding element equations.

Following the trivial FEM global equation assembly, it follows that the global form of the equations discussed above is:

$$M_G\ddot{X} + C_G\dot{X} + K_G X = \tilde{F} \quad (41)$$

, where:

- $M_G,\ C_G,\ K_G$ are global square matrices of $(3n \times 3n)$ dimensions, with n denoting the total number of node points in the structure.
- $X = \{x_1,\ y_1,\ z_1,\ x_2,\ y_2,\ z_2,\ x_3,\ y_3,\ z_3,\ \cdots\}^T$ is the global displacement vector of $(3n \times 1)$ dimension.
- $\tilde{F} = F + F_u$, with F denoting the sum of forces of the unforced problem and F_u being the force input to the system (typically at one or both ends of the cable structure).

As stated in the introduction of the thesis, we wish to transform the above derived equations to a form resembling a control scheme. To that end, declaring the nodal displacements and velocities as state variables, one can write:

$$\begin{aligned} &\dot{x} = \dot{x} \\ &\ddot{x} = -M_G^{-1}C_G\dot{x} - M_G^{-1}K_G x + M_G^{-1}\tilde{F} \end{aligned} \quad (42)$$

Writing the above equations to matrix form, it follows that:

$$\begin{bmatrix} \dot{x} \\ \ddot{x} \end{bmatrix} = \begin{bmatrix} 0 & I \\ -M_G^{-1}K_G & -M_G^{-1}C_G \end{bmatrix}\begin{bmatrix} x \\ \dot{x} \end{bmatrix} + \begin{bmatrix} 0 \\ M_G^{-1} \end{bmatrix}\tilde{F} \quad (43)$$

, or in other words:

$$\dot{y} = Ay + Bu \quad (44)$$

Appendix

A. Local coordinate system definition

The calculations performed in order to define the local coordinate system are presented here. The standard coordinate transformation matrix T in the FEM is defined as follows:

$$T_{G2L} = \begin{bmatrix} c_y c_z & c_y s_z & -s_y \\ -c_x s_z + s_x s_y c_z & c_x c_z + s_x s_y s_z & s_x c_y \\ s_x s_z + c_x s_y c_z & -s_x c_z + c_x s_y s_z & c_x c_y \end{bmatrix} \quad (45)$$

When expressed in terms of the body fixed frame, the only non-zero component of the length vector is in the x direction. Thus, it follows that:

$$\begin{bmatrix} dx \\ dy \\ dz \end{bmatrix} = T_{L2G} \begin{bmatrix} L \\ 0 \\ 0 \end{bmatrix} \quad (46)$$

This results into the following:

$$Lc_y c_z = dx$$
$$Lc_y s_z = dy$$
$$-Ls_y = dz$$

Given the known initial state of the umbilical tether, the values of dx, dy, dz are known. The length L can be calculated anytime as:

$$L = \sqrt{dx^2 + dy^2 + dz^2}$$

With minor equation manipulation, the values of angles about y and z axis can be derived:

$$\theta_z = \tan 2^{-1}(dy, dx)$$

$$(c_z > s_z) \begin{cases} \text{true} \Rightarrow \theta_y = \tan 2^{-1}\left(-dz, \dfrac{dx}{c_z}\right) \\ \text{false} \Rightarrow \theta_y = \tan 2^{-1}\left(-dz, \dfrac{dy}{s_z}\right) \end{cases}$$

All that remains now in order for the local coordinate system to be fully defined is to find θ_x. By theory, the system was defined in such a way that the fluid velocity relative to the element in the local coordinates can be written as:

$$v = \dot{r} - v_c = \begin{bmatrix} \dot{x} - v_{cx} & \dot{y} - v_{cy} & 0 \end{bmatrix}^T \quad (47)$$

The following equation holds:

$$\vec{v} = R_{G2L}\vec{u} \Rightarrow \begin{bmatrix} v_x \\ v_y \\ 0 \end{bmatrix} = R_{G2L} \begin{bmatrix} u_x \\ u_y \\ u_z \end{bmatrix} \quad (48)$$

The 3rd equation provides the value of dx. More specifically:

$$\begin{bmatrix} s_x s_z + c_x s_y c_z & -s_x c_z + c_x s_y s_z & c_x c_y \end{bmatrix} \begin{bmatrix} u_x \\ u_y \\ u_z \end{bmatrix} = 0 \quad (49)$$

Given the known initial state of the tether, the vector of global nodal velocities $\vec{u}$ is known as well. This leads to the following system of equations:

$$\begin{aligned} & s_x \left(s_z u_x - c_z u_y \right) + c_x \left(s_y c_z u_x + s_y s_z u_y + c_y u_z \right) = 0 \\ & s_x^2 + c_x^2 = 1 \end{aligned} \quad (50)$$

The solution of this system yields the values of $\sin\theta_x$, $\cos\theta_x$ and fully defines the local coordinate system.

B. Rayleigh damping constants calculation

The modes of the system are solutions to the homogenous form of the equations, which are written as:

$$\left(\left[M\right]p^2+\left[C\right]p+\left[K\right]\right)\{\varphi\}=\{0\} \quad (51)$$

$$p=-\sigma+j\dot{\omega} \quad (19)$$

Substituting (51) into (52) and rearranging terms gives:

$$\begin{aligned}&\left(\left[M\right]p^2+\left(\alpha\left[M\right]+\beta\left[K\right]\right)p+\left[K\right]\right)\{\varphi\}=\{0\}\Rightarrow\dots\\&\left(\left[M\right]\left(\left(\sigma^2-\omega-\alpha\sigma\right)+j\left(-2\sigma\omega+\alpha\omega\right)\right)+\left[K\right]\left(\left(-\sigma\beta+1\right)+j\beta\omega\right)\right)\{\varphi\}=\{0\}\end{aligned} \quad (53)$$

A known property of the mode shapes $\{\varphi\}$ of an undamped structure model is that they are real valued. This means that the real and imaginary parts of (53) are uncoupled, and therefore can be rewritten as separate equations:

$$\begin{aligned}&\left(\left[M\right]\left(\sigma^2-\omega^2-\alpha\sigma\right)+\left[K\right]\left(-\sigma\beta+1\right)\right)\{\varphi\}=\{0\}\\&\left(\left[M\right]\left(-2\sigma\omega-\alpha\omega\right)+\left[K\right]\beta\omega\right)\{\varphi\}=\{0\}\end{aligned} \quad (54)$$

Putting these equations in the standard form for an undamped structure yields:

$$\begin{aligned}&\left(\frac{\left(\sigma^2-\omega^2-\alpha\sigma\right)}{-\sigma\beta+1}\left[M\right]+\left[K\right]\right)\{\varphi\}=\{0\}\\&\left(\frac{\left(-2\sigma+\alpha\right)}{\beta}\left[M\right]+\left[K\right]\right)\{\varphi\}=\{0\}\end{aligned} \quad (55)$$

Both of these equations must be satisfied for a proportionally damped structure. The solutions to this equation are unique poles. The equation for each pole can be written as:

$$\begin{aligned}&\frac{\left(\sigma^2-\omega^2-\alpha\sigma\right)}{\left(-\sigma\beta+1\right)}=\frac{\left(-2\sigma+\alpha\right)}{\beta}=-\Omega^2\\&\Omega^2=\sigma^2+\omega^2\end{aligned} \quad (56)$$

, where Ω is an undamped natural frequency. This provides a single equation with two unknowns (α and β):

$$2\sigma=\alpha+\beta\left(\sigma^2+\omega^2\right) \quad (57)$$

Given a set of EMA frequencies and damping for n modes ($n\geq 2$), n equations can be written:

$$2\begin{Bmatrix}\sigma_1\\ \sigma_2\\ \vdots\\ \sigma_n\end{Bmatrix}=\begin{bmatrix}1 & \Omega_1^2\\ 1 & \Omega_2^2\\ \vdots & \vdots\\ 1 & \Omega_n^2\end{bmatrix}\begin{Bmatrix}\alpha\\ \beta\end{Bmatrix} \quad (58)$$

The least-squared solution of the overdetermined system presented above yields approximate values for the damping coefficients.

As for the natural frequencies themselves, they can be derived by solving the following eigenvalue problem for the undamped, unforced structure:

$$\left(\left[M\right]\omega^2+\left[K\right]\right)\left\{X\right\}=\left\{0\right\} \quad (59)$$

C. Fluid velocity

The global current profile imposed during this thesis is a complex 2-d current profile, given by the following equation:

$$\vec{U}=u\cos\left(\frac{2\pi z}{h}\right)\vec{I}+u\sin\left(\frac{2\pi z}{h}\right)\vec{J} \quad (60)$$

, where:

- z is the corresponding coordinate of the point under consideration in the z-axis.
- h is the maximum water depth

As is apparent, the sheared current velocity is a function of the depth only, and there is no vertical component of the current. However, the program developed allows the user to impose a constant potential vertical percussive value to simulate a disturbance of the form of a wave in the z direction in case this is desirable.

Chapter 4
Simulation Results

In order to verify the performance of the script written in Matlab, we tried to reproduce the results of experiments presented at [17] and used as verification data in [1]. These experiments' scenario specified the upper end's displacement and velocity profiles resembling a straight unsteady tow operation.

The experiments that were used for the validation process were of 2 kinds:

- Acceleration test: For the straight tow considered here, the motion of the towpoint is constrained to the X axis of the inertial frame and is defined by the piecewise function defined as follows:

Time (s)	$\dot{r}_X^{(0)}$ *(m/s)*	$r_X^{(0)}$ *(m)*
$0.0 < t \leq 120.0$	0.566	$0.566 \cdot t$
$120.0 < t \leq 180.0$	$0.566 + 0.0112 \cdot (t - 120)$	$67.92 + 0.566 \cdot (t - 120) + 0.006 \cdot (t - 120)^2$
$180.0 < t$	1.235	$123.48 + 1.235 \cdot (t - 180)$

The towpoint motion corresponds to a cruise speed of 0.566 m/s for a 120s interval. During this time the cable achieves an equilibrium profile. Since the material properties are uniform over the scope of the cable, the equilibrium profile is expected to be a straight line inclined to the free surface. After that, an acceleration period of 60s occurs, during which the towpoint achieves linearly a speed of 1.235 m/s, which remains constant for the rest of the duration of the experiment.

- Deceleration test: Once again, the motion of the towpoint is constrained to the X axis of the inertial frame and is defined by the following piecewise function

Time (s)	$\dot{r}_X^{(0)}$ *(m/s)*	$r_X^{(0)}$ *(m)*
$0.0 < t \leq 60.0$	1.286	$1.286 \cdot t$
$60.0 < t \leq 120.0$	$1.286 - 0.0129 \cdot (t - 60)$	$77.16 + 1.286 \cdot (t - 60) - 0.0065 \cdot (t - 60)^2$
$120.0 < t$	0.514	$131.2 + 0.514 \cdot (t - 120)$

The physical properties of the cable were the same as those that were used in [17] and are summarized in the following table:

Parameter	*Symbol*	*Value*
Cable diameter	d_c	0.0332 m
Cable density	ρ_c	3121 kg/m^3
Effective modulus of elasticity	E	77.5 GPa
Cable length	L	300 m

The results derived from simulating with the above kinematic constraints, using 6 elements of 50m length, are shown in the plot diagrams that follow:

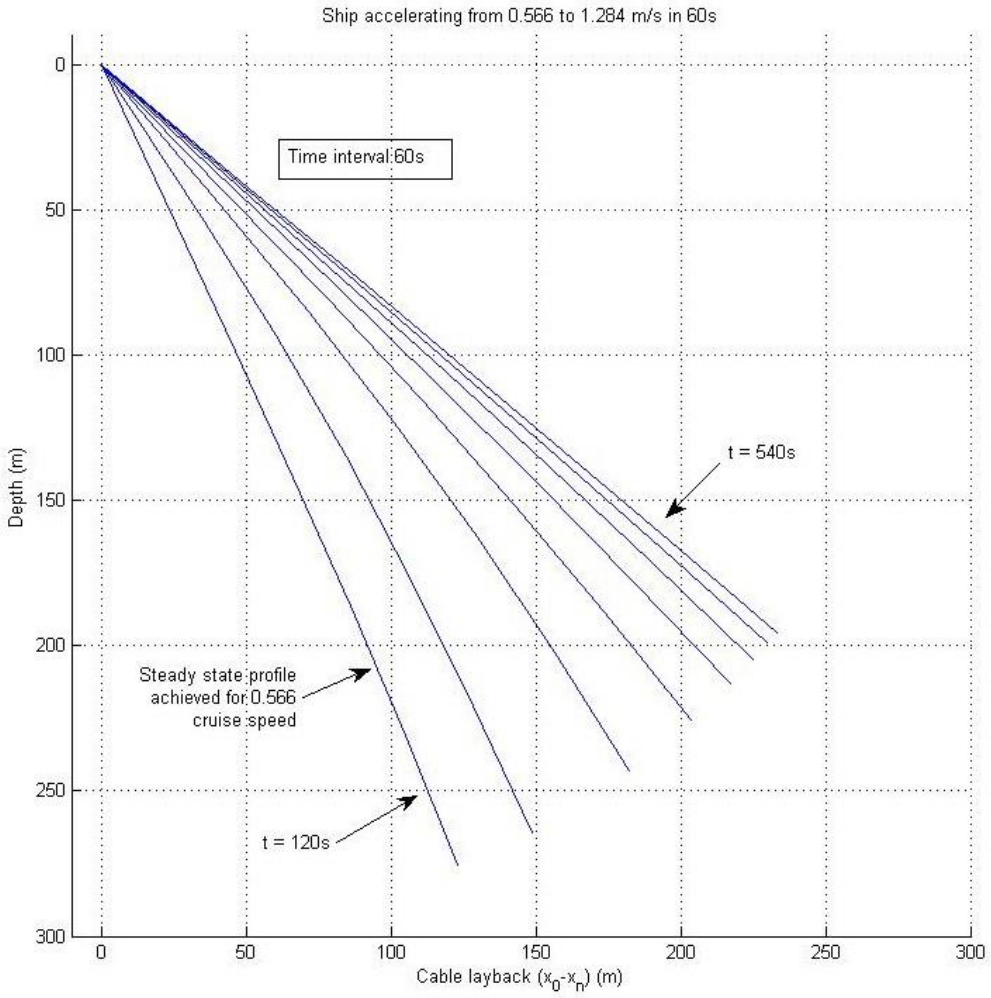

Figure 4. Tether attached to ship, ship accelerating from 0.566 to 1.284 m/s

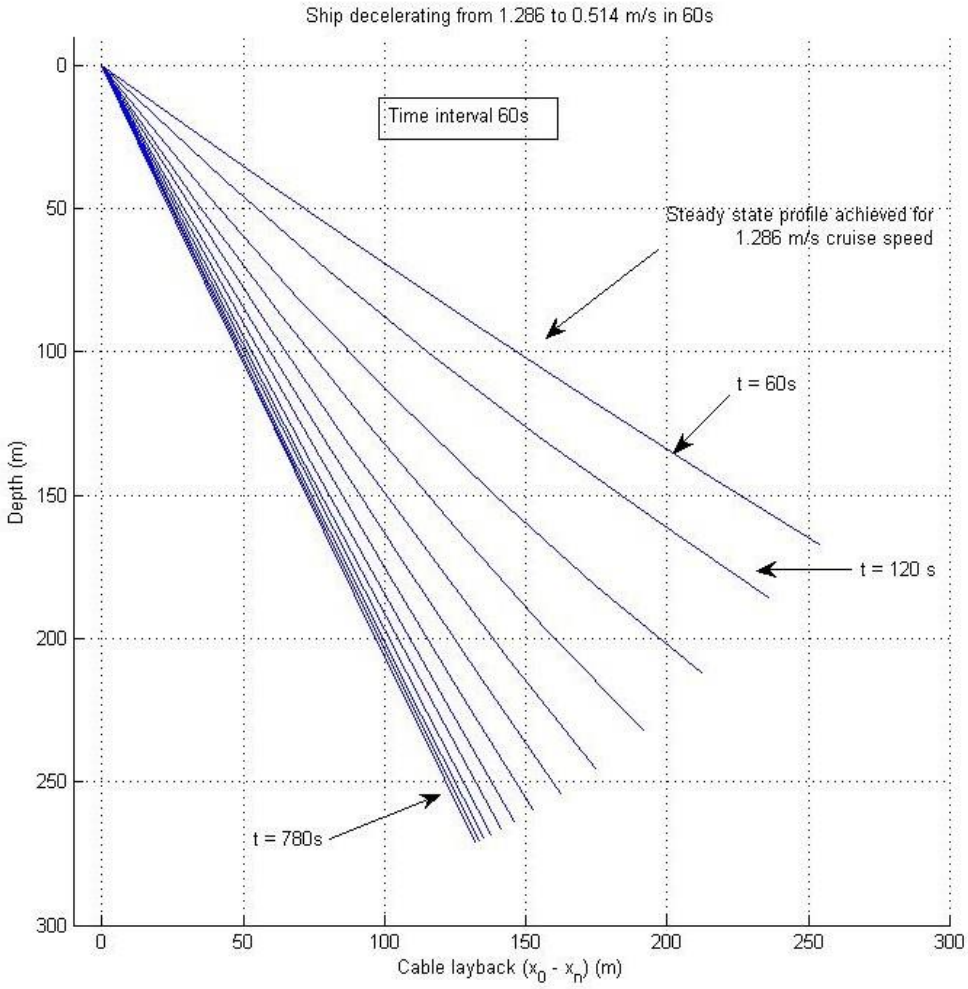

Figure 5. Tether attached to ship, ship decelerating from 1.286 to 0.514 m/s

The experiments used to validate the model and the corresponding code in Matlab assumed excitation of the system in terms of kinematic constraints at the upper end. To further investigate the performance of the code, additional simulations were conducted that assumed dynamic constraints at either one, or both ends of the umbilical tether. These are relevant to operating scenarios during which a ROV is attached to the lower end of the tether, while the upper end is firmly attached to the surface station (i.e. a boat).

In particular, three operating cases were considered during this thesis:

1. Stationary upper end (equivalent to an anchor), with a constant known force applied at the lower end. This is the most common scenario that one will face in real life operations. Typically, the surface station will be stationary and the ROV will perform whatever task the engineer wants it to do.
2. Stationary lower end and a constant known force applied at the upper end.
3. Both ends movable, with constant, equal and opposite forces applied at both ends.

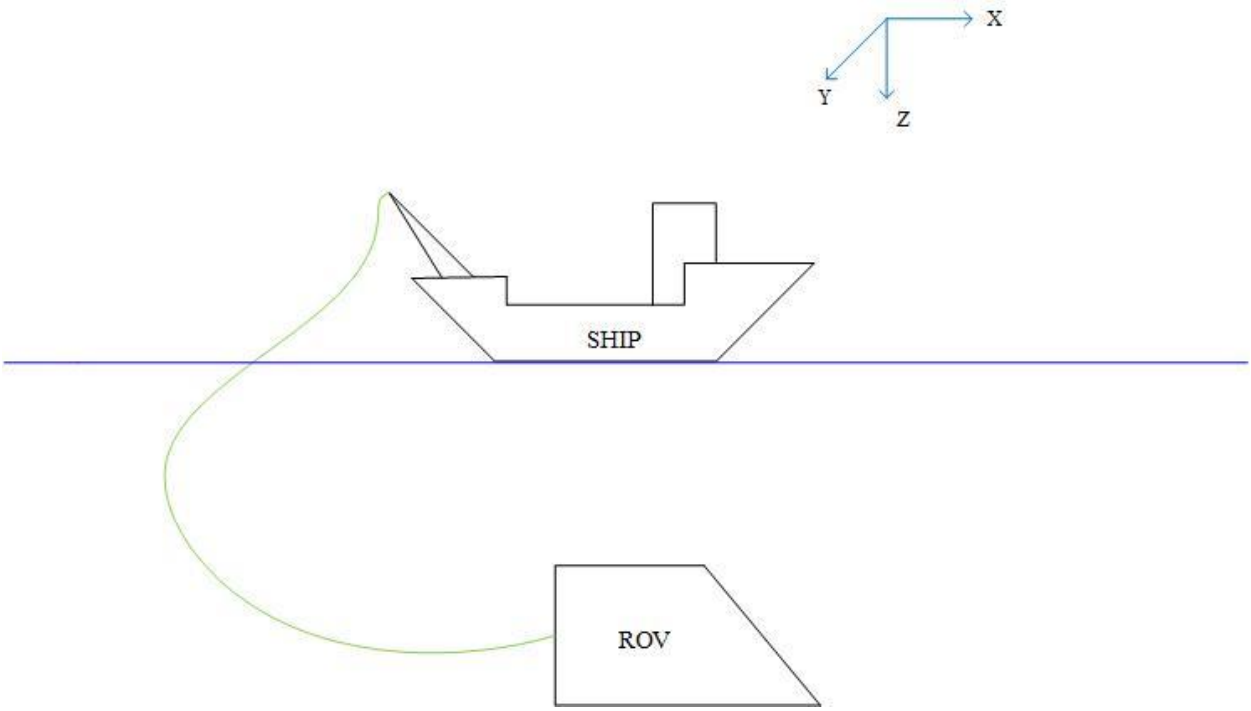

Figure 6. General configuration of a ROV attached to a ship

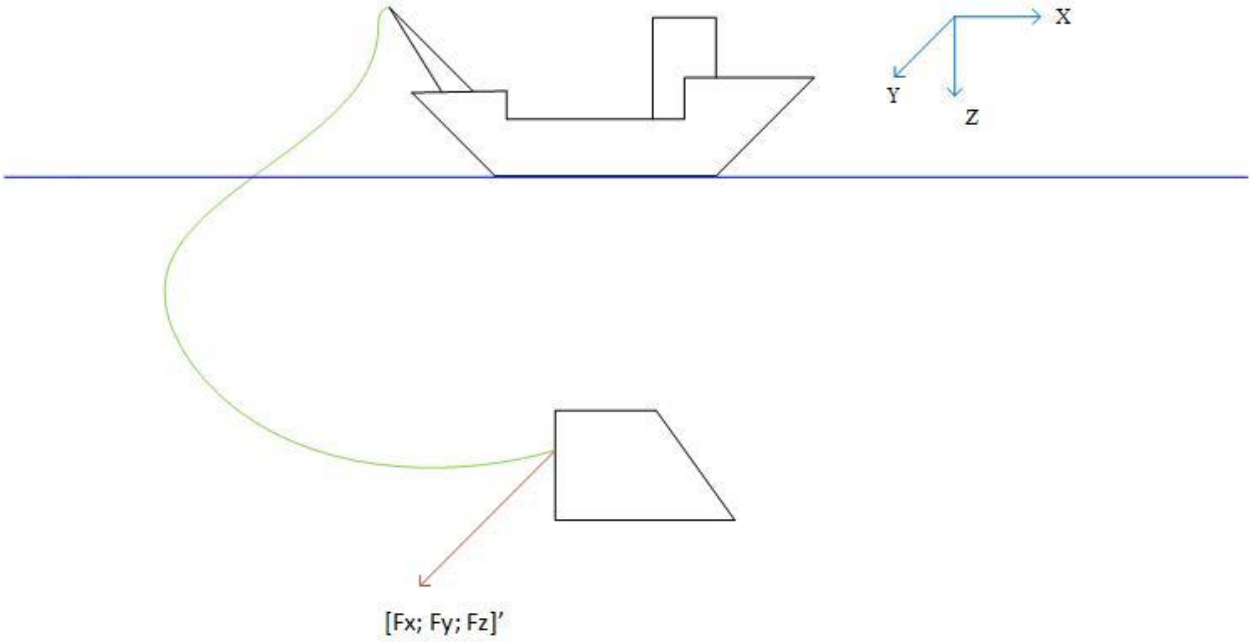

Figure 7. Operating scenario #1 schematic

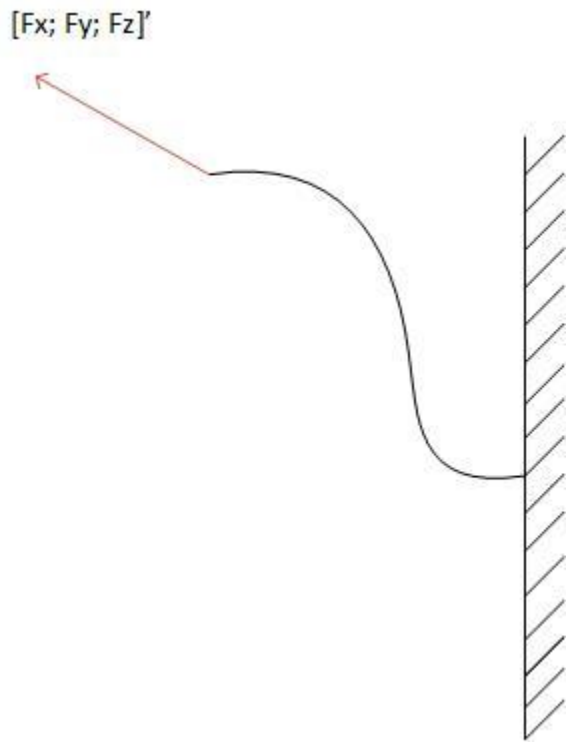

Figure 8. Operating scenario #2 schematic

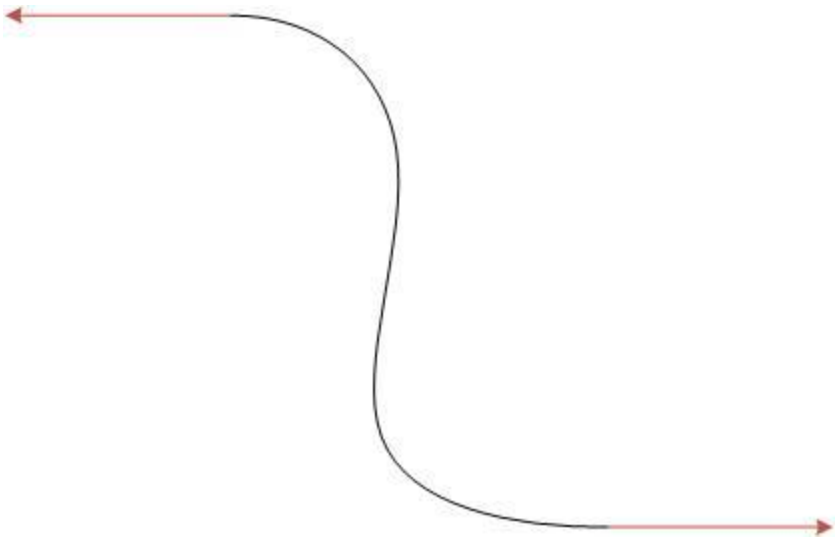

Figure 9. Operating scenario #3 schematic

These scenarios were simulated for varying environmental conditions and disturbances. In general, surface ocean currents are driven by the wind and the velocity drops off rapidly with depth. For example, the Gulf Stream appears to be the fastest with reported speeds of up to 2.5 meters per second (5.4 miles per hour). However the average surface velocity of the Gulf Stream is less than 1 meter per second and other surface currents are even slower. Deep water currents are driven by temperature and salinity differences and are slower still - generally less than 0.01 meters per second.

Taking all of the above into account, simulations were performed under the assumption of absence of current, and the presence of currents of 0.5m/s and 1m/s amplitudes, which resemble conditions close to typical ones. During the simulations, discretization of 10 elements with universal properties and equal starting length was used. The driving force was taken to be $F = [100 \quad 30 \quad 0]\,(N)$ unless otherwise mentioned. The cable attributes and the results are summarized below:

Parameter	*Symbol*	*Value*
Cable diameter	d_c	0.0332 m
Cable density	ρ_c	1200 kg/m^3
Effective modulus of elasticity	E	77.5 MPa
Cable length	L	100 m

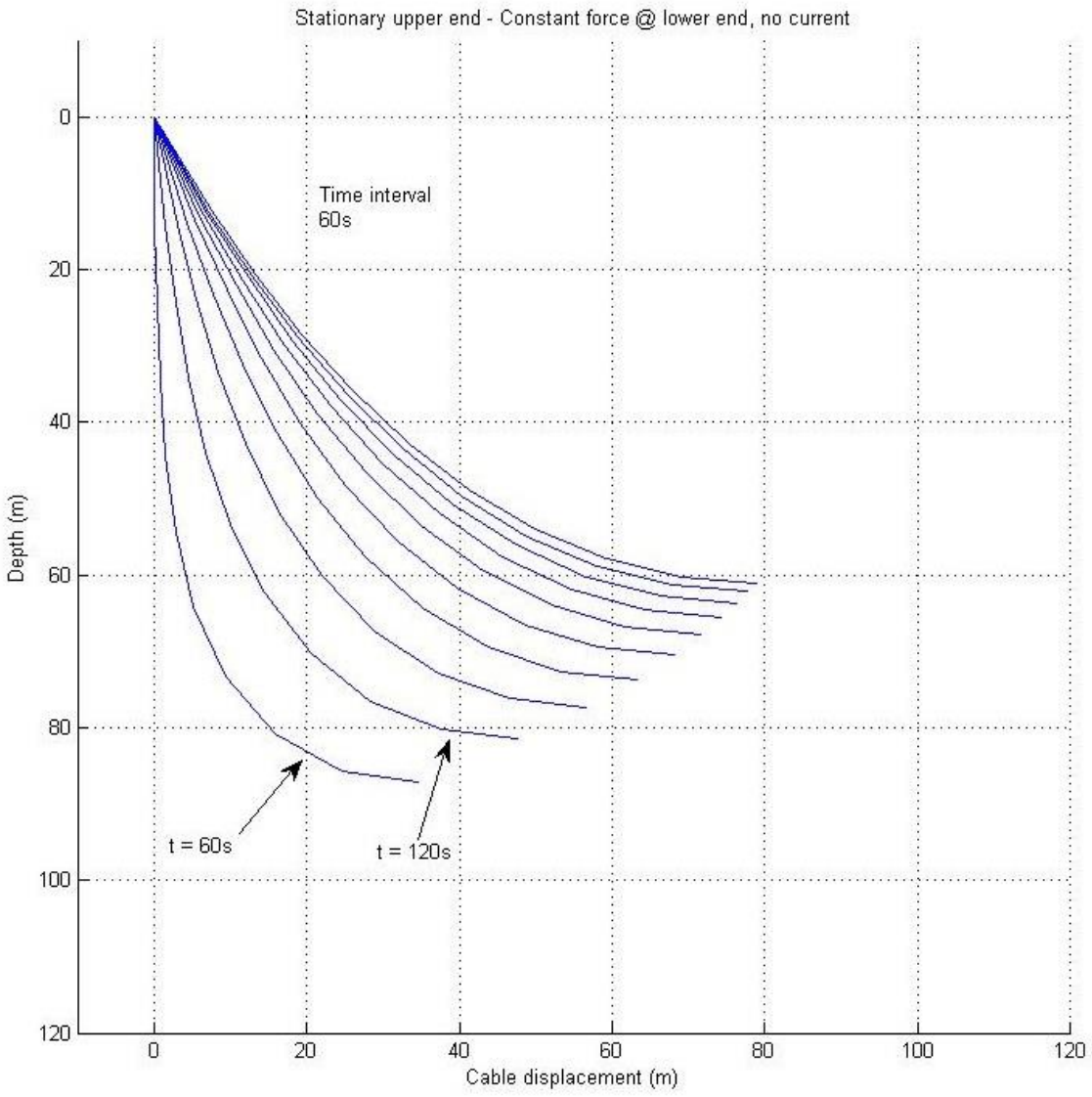

Figure 10. Stationary upper end, no current

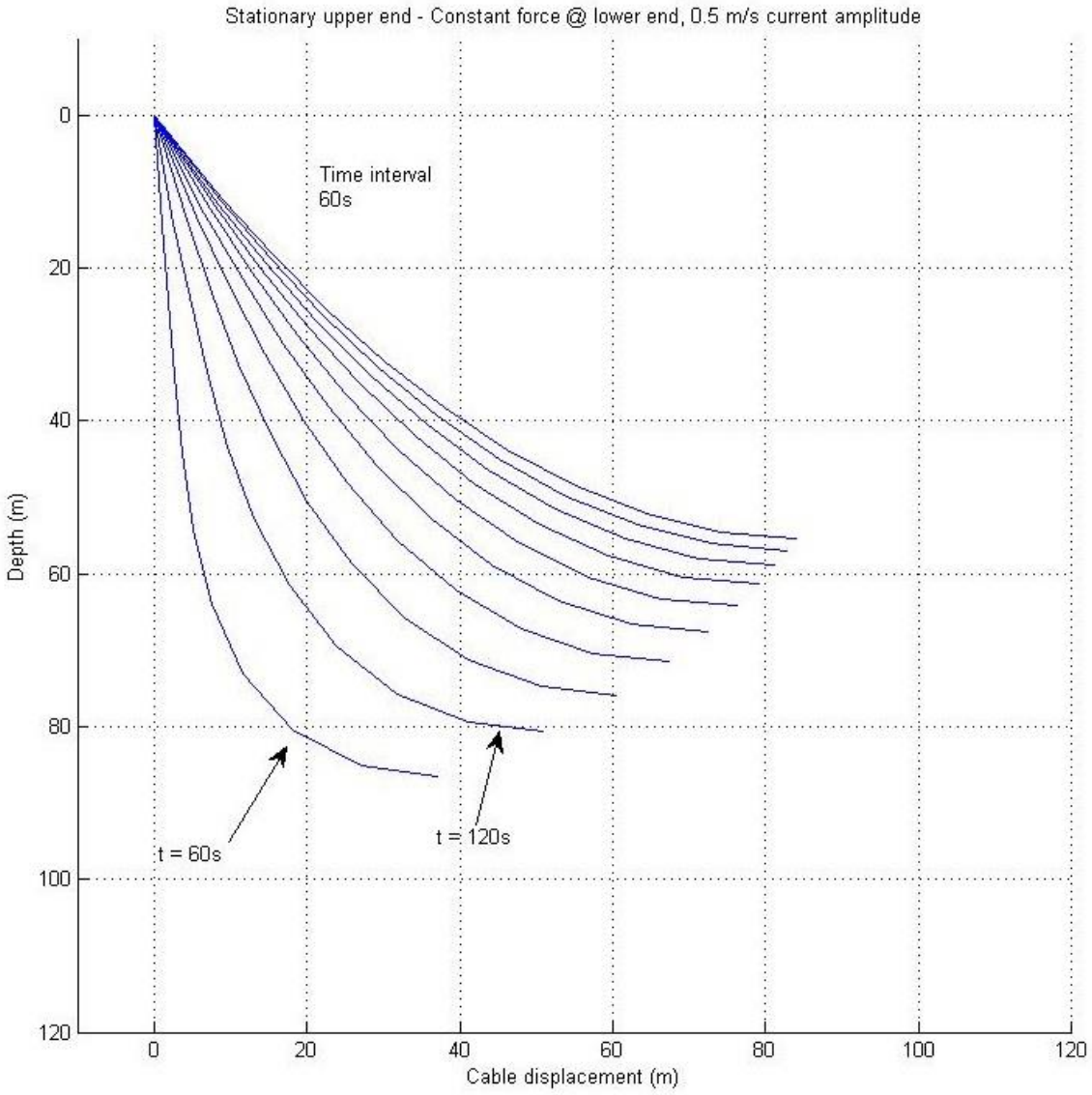

Figure 11. Stationary upper end, 0.5 m/s current amplitude

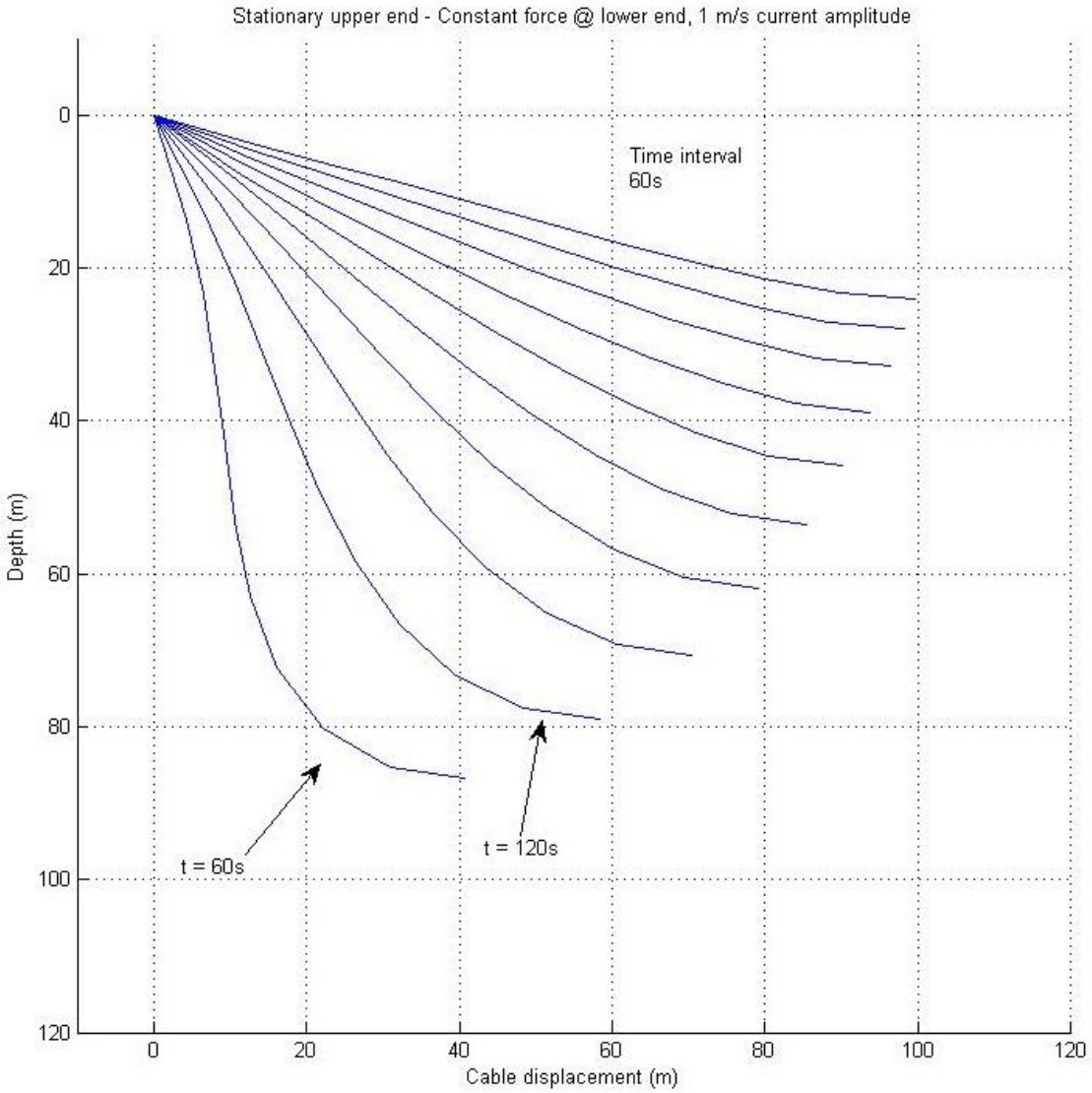

Figure 12. Stationary upper end, 1 m/s current amplitude

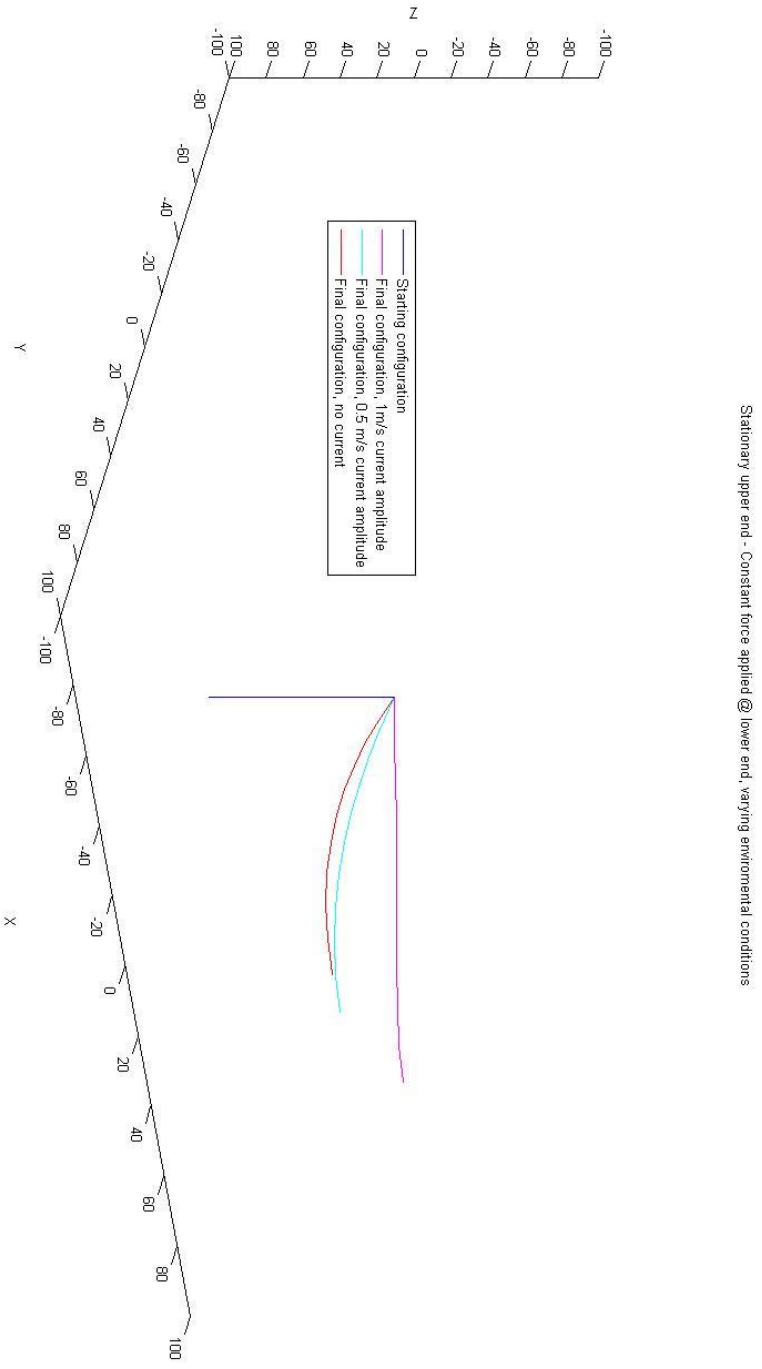

Figure 13. Projection of final configurations w.r.t starting configuration

Further simulations were conducted assuming an equal but opposite force at the lower end in comparison with the previous case. The results are displayed below:

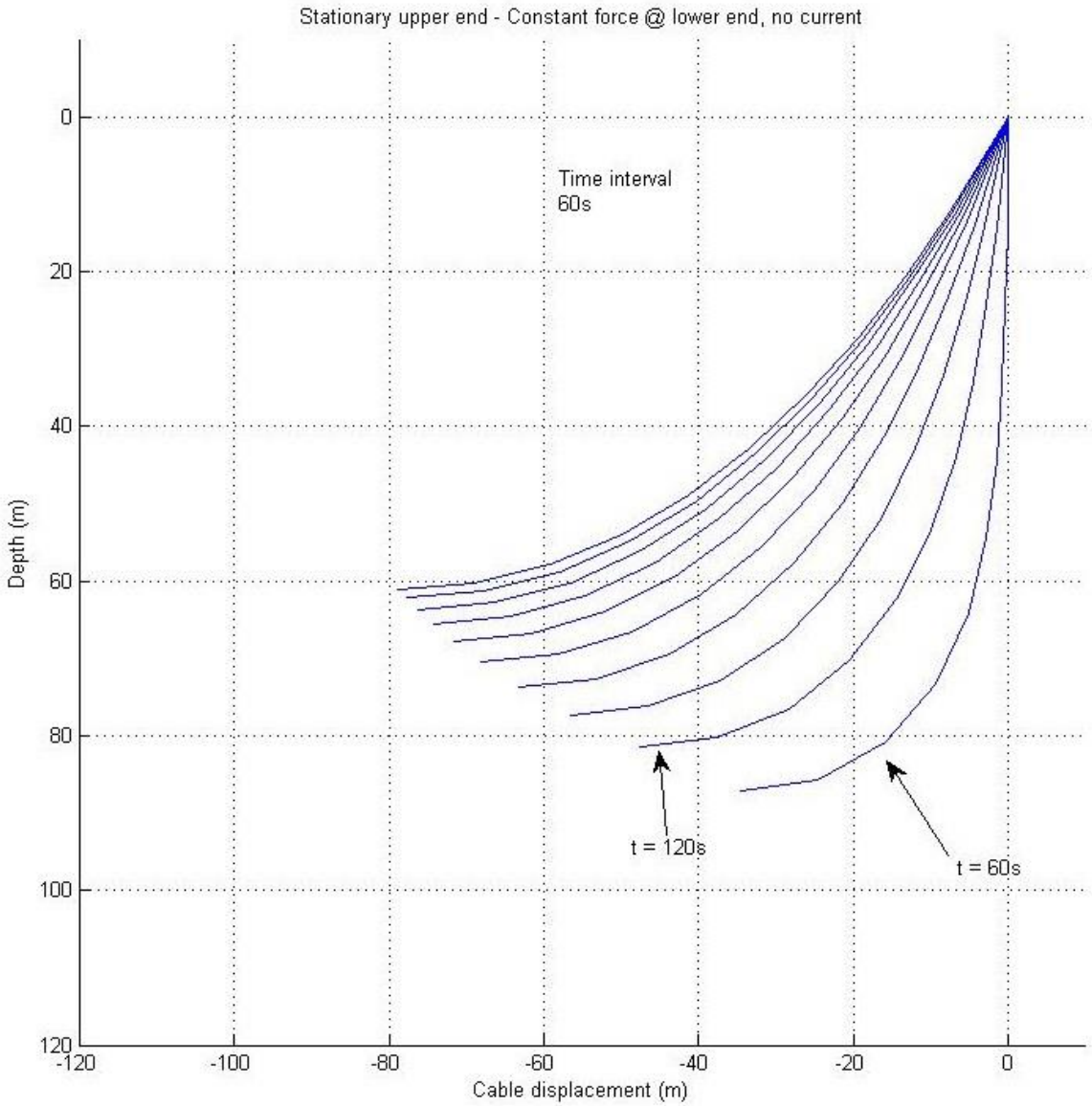

Figure 14. Stationary upper end, equal and opposite force at lower end, no current

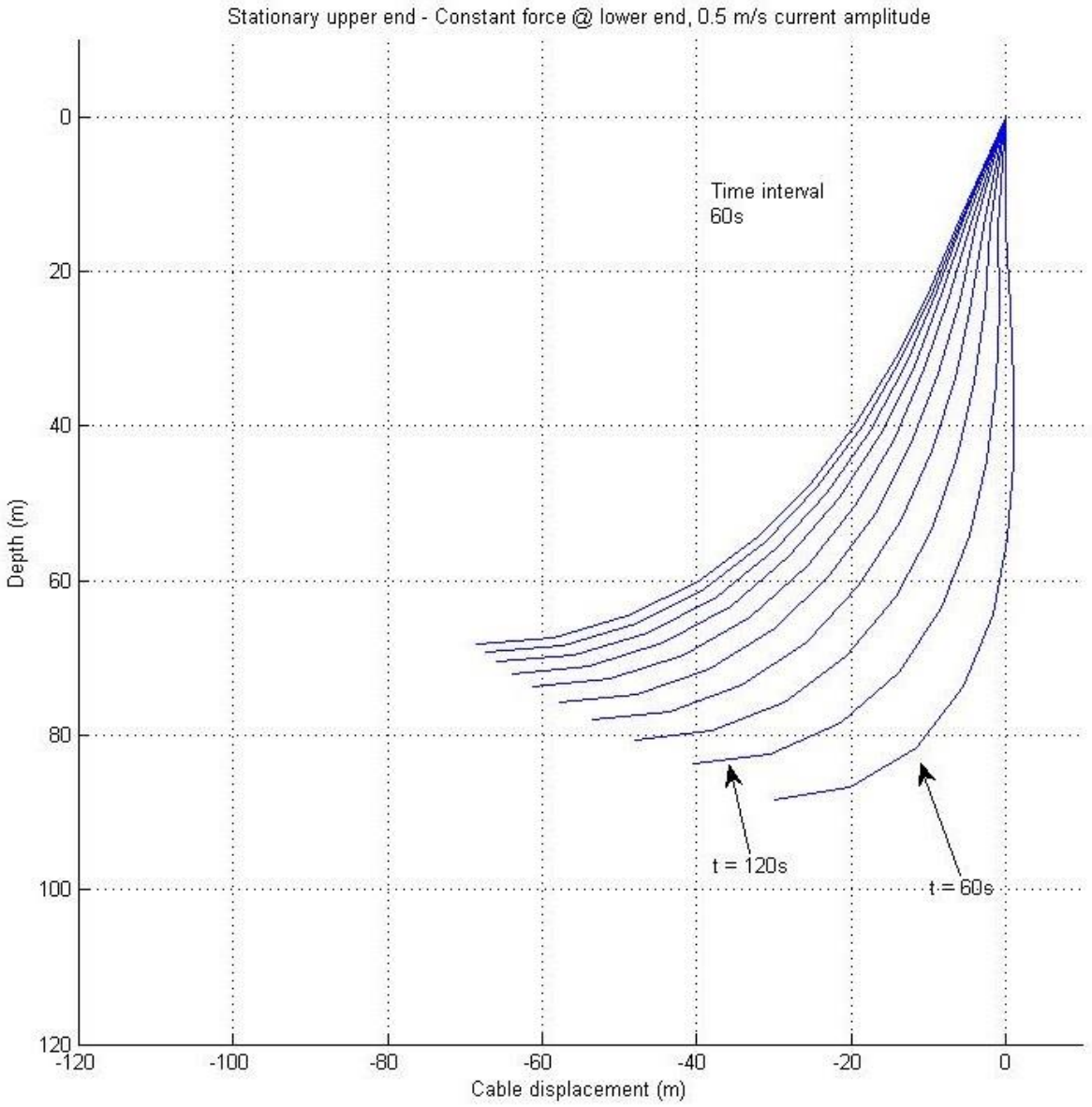

Figure 15. Stationary upper end, equal and opposite force at lower end, 0.5 m/s current amplitude

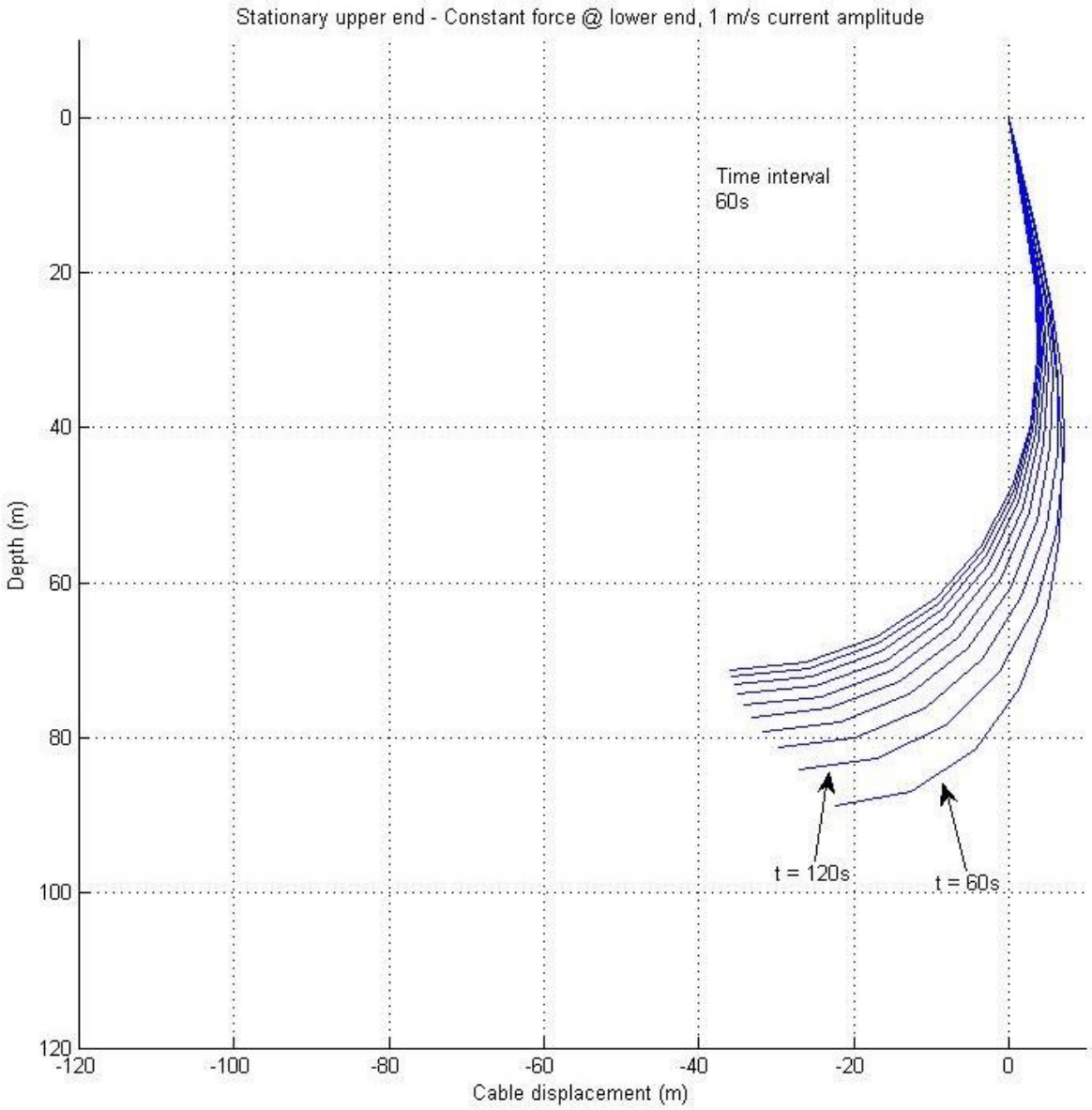

Figure 16. Stationary upper end, equal and opposite force at lower end, 11 m/s current amplitude

In order to verify the model's performance, the above displayed results were compared with the corresponding ones for a cable with the same attributes except for its density, which was taken to be equal to 1600 kg/m^3. This resulted to the cable becoming heavier, thus affecting its' dynamic response. The excitation force at the lower end of the cable remained the same during these simulations. The results are displayed below:

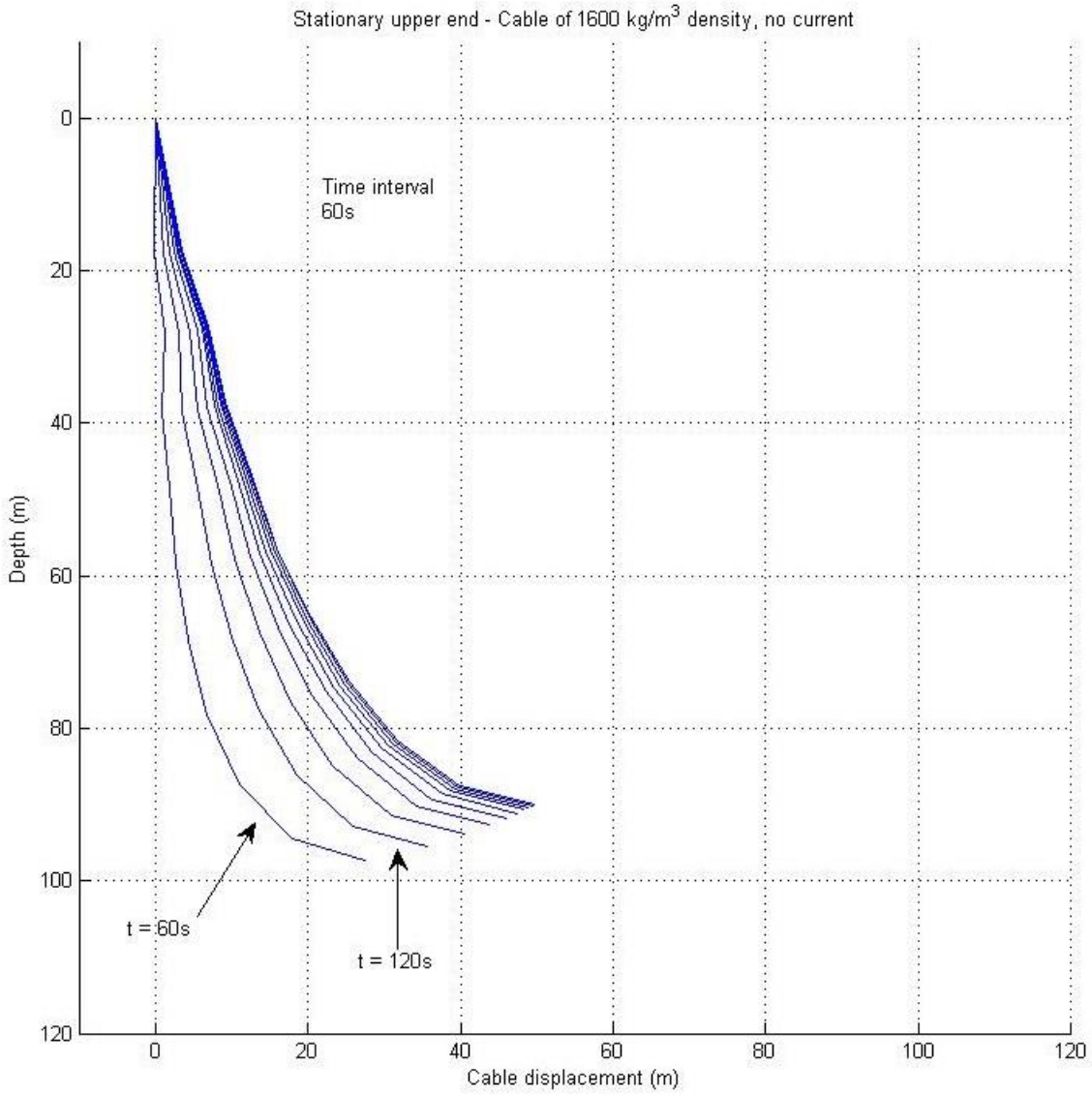

Figure 17. Stationary upper end, 1600 kg/m^3 cable density, no current

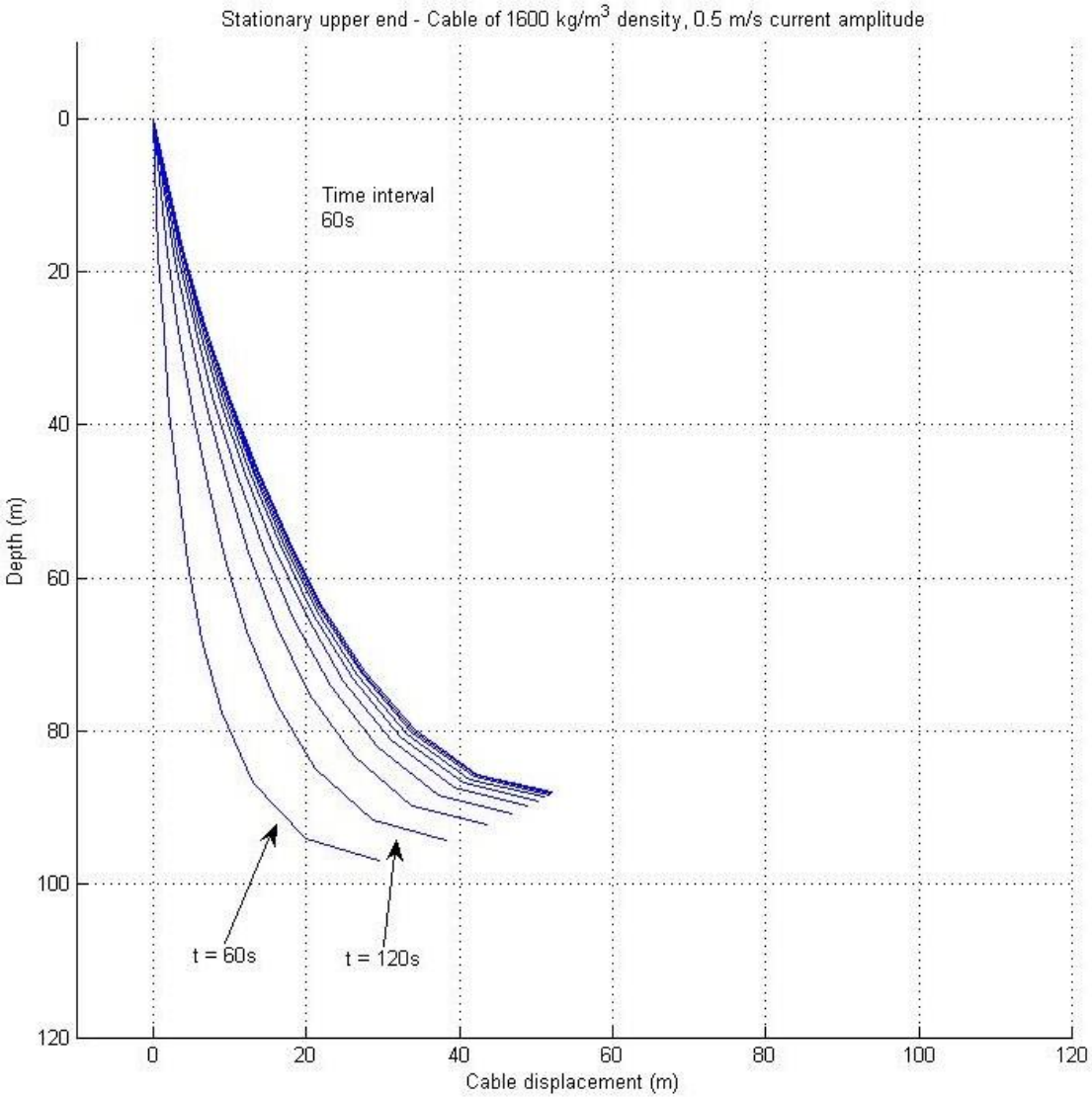

Figure 18. Stationary upper end, 1600 kg/m^3 cable density, current amplitude 0.5 m/s

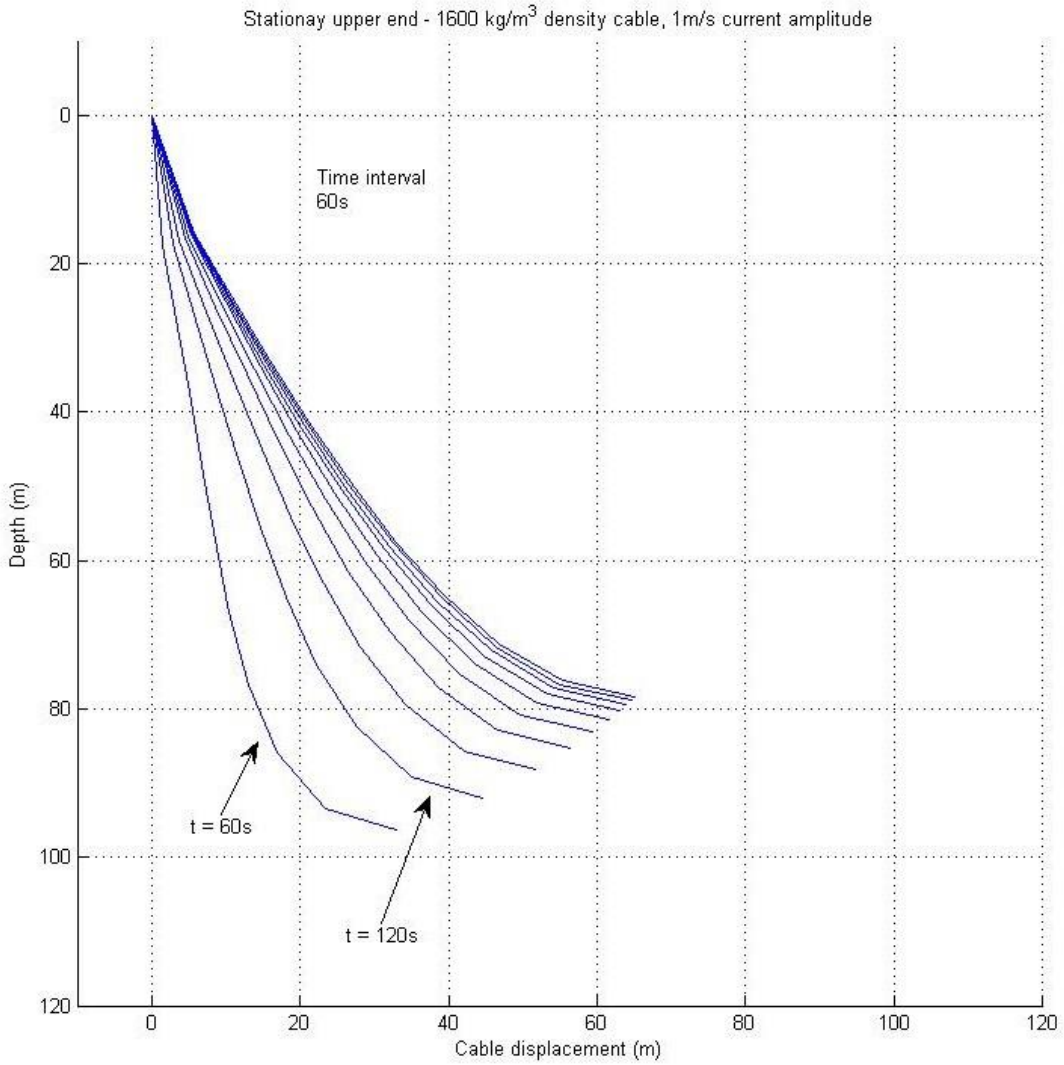

Figure 19. Stationary upper end, 1600 kg/m^3 cable density, current amplitude 1m/s

We can see that the results indeed depict the expected performance of the umbilical. With its density changed it became heavier, thus the excitation force has a lesser impact on its shape. More specifically, it is more difficult for the upper part of the cable to follow the motion indicated by the lower part. Also, the environmental disturbances tend to affect it less than the previous case.

Results from operating scenarios 2 and 3 are displayed in the plots that follow:

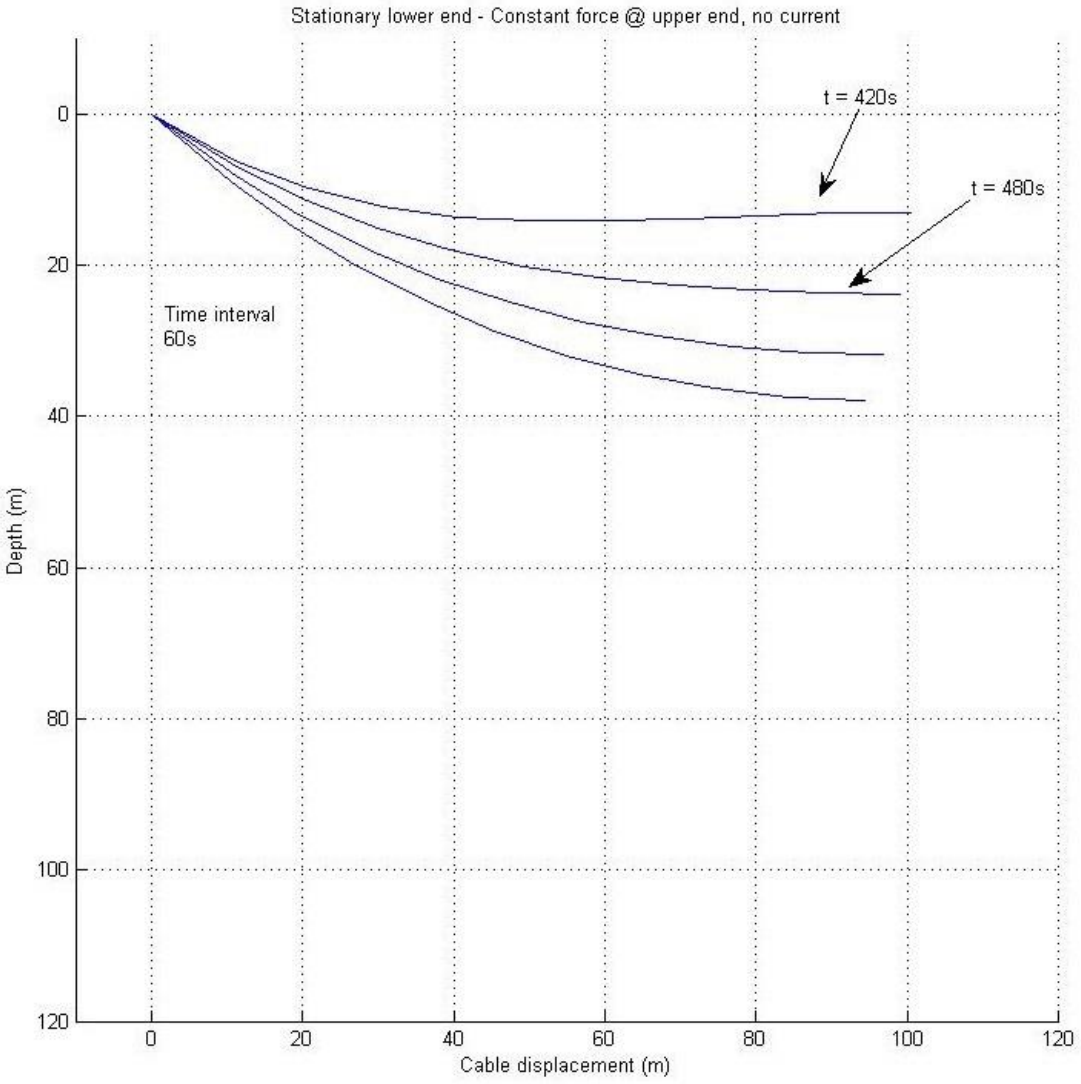

Figure 20. Stationary lower end, no current

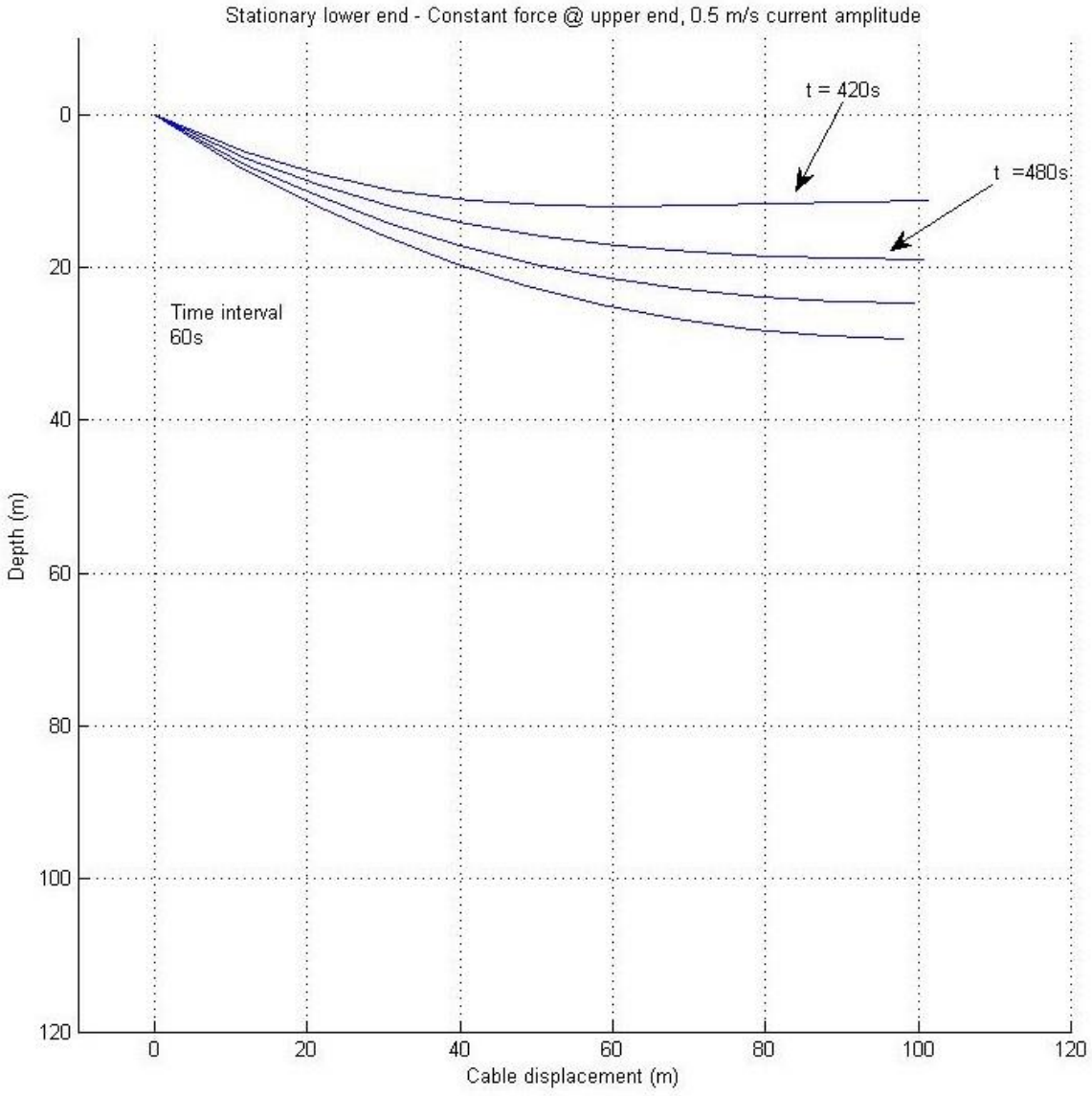

Figure 21. Stationary lower end, current amplitude 0.5 m/s

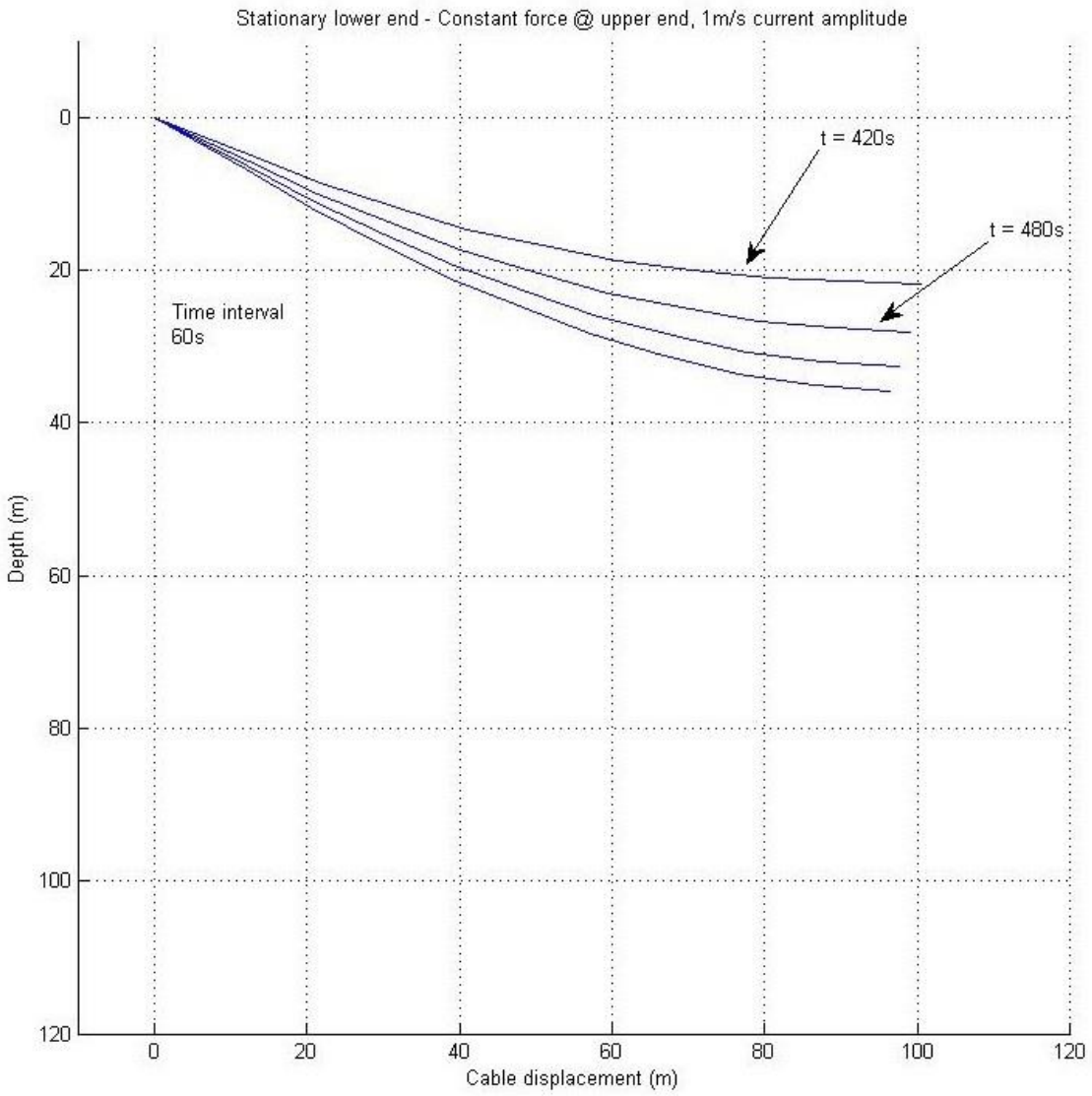

Figure 22. Stationary lower end, current amplitude 1m/s

During this operating scenario, the gravity is the dominant force over the entire cable length. The cable shapes of time before the mark of 420s were omitted, since during that period the cable is performing a snake-like motion while descending. The inclusion of such shapes would have rendered the resulting plot incomprehensible for the reader.

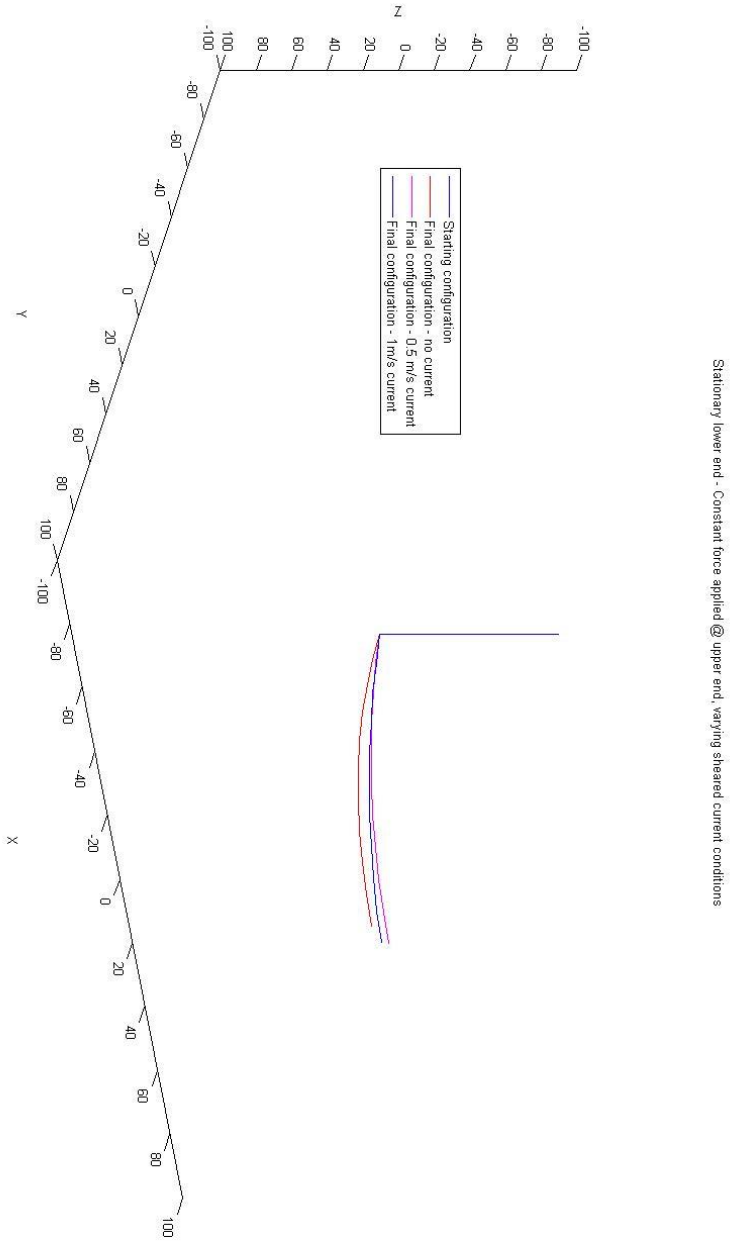

Figure 23. Projection of final configurations w.r.t starting configuration

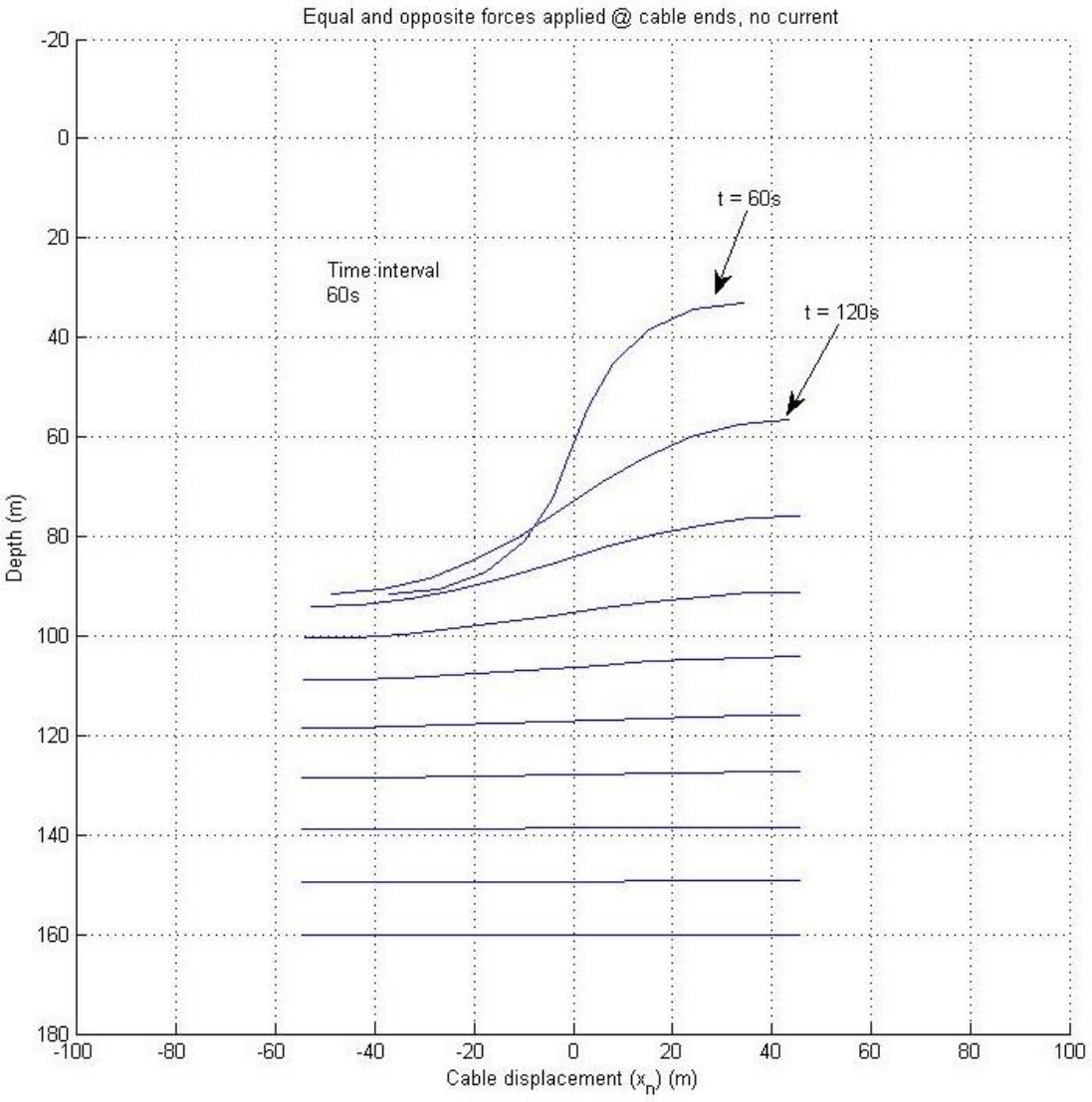

Figure 24. Equal and opposite forces at both ends, no current

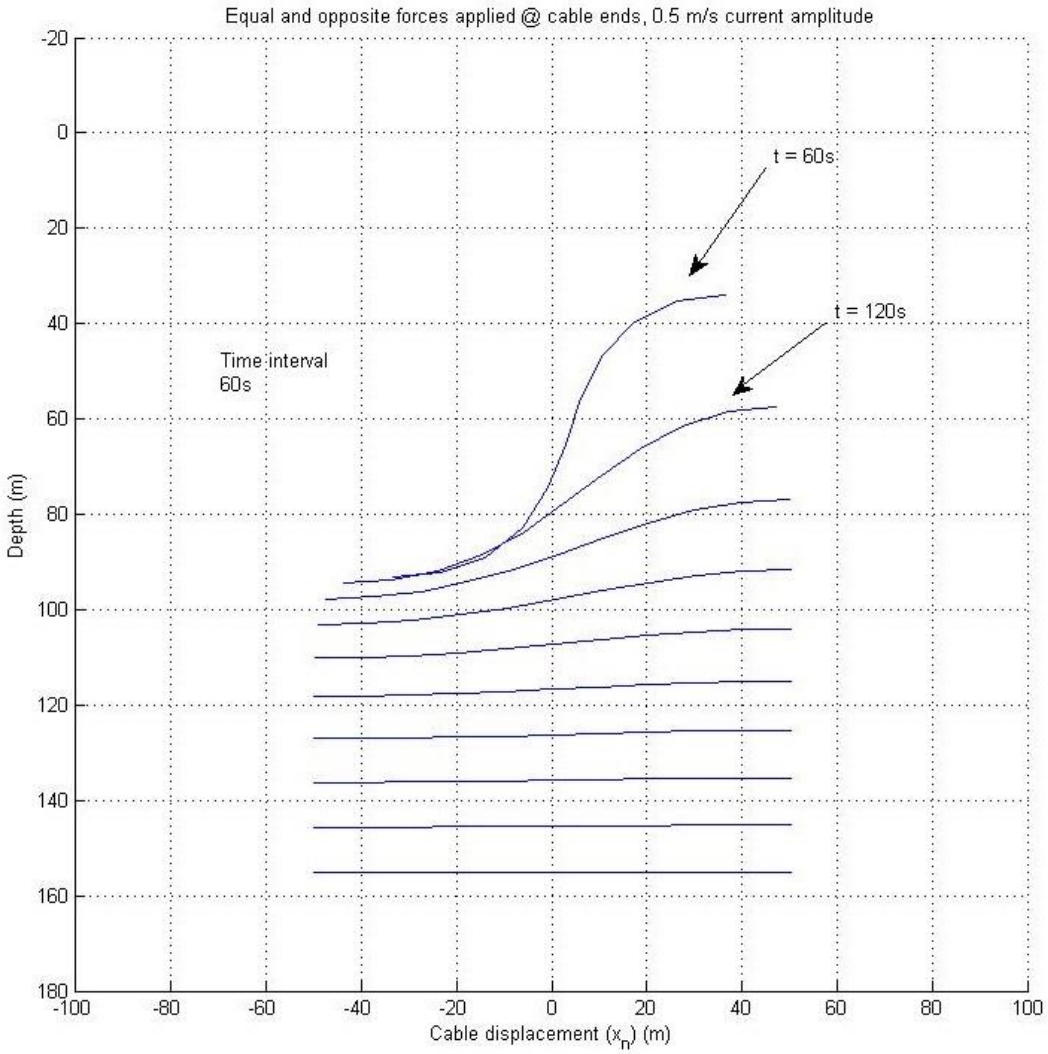

Figure 25. Equal and opposite forces at both ends, current amplitude 0.5 m/s

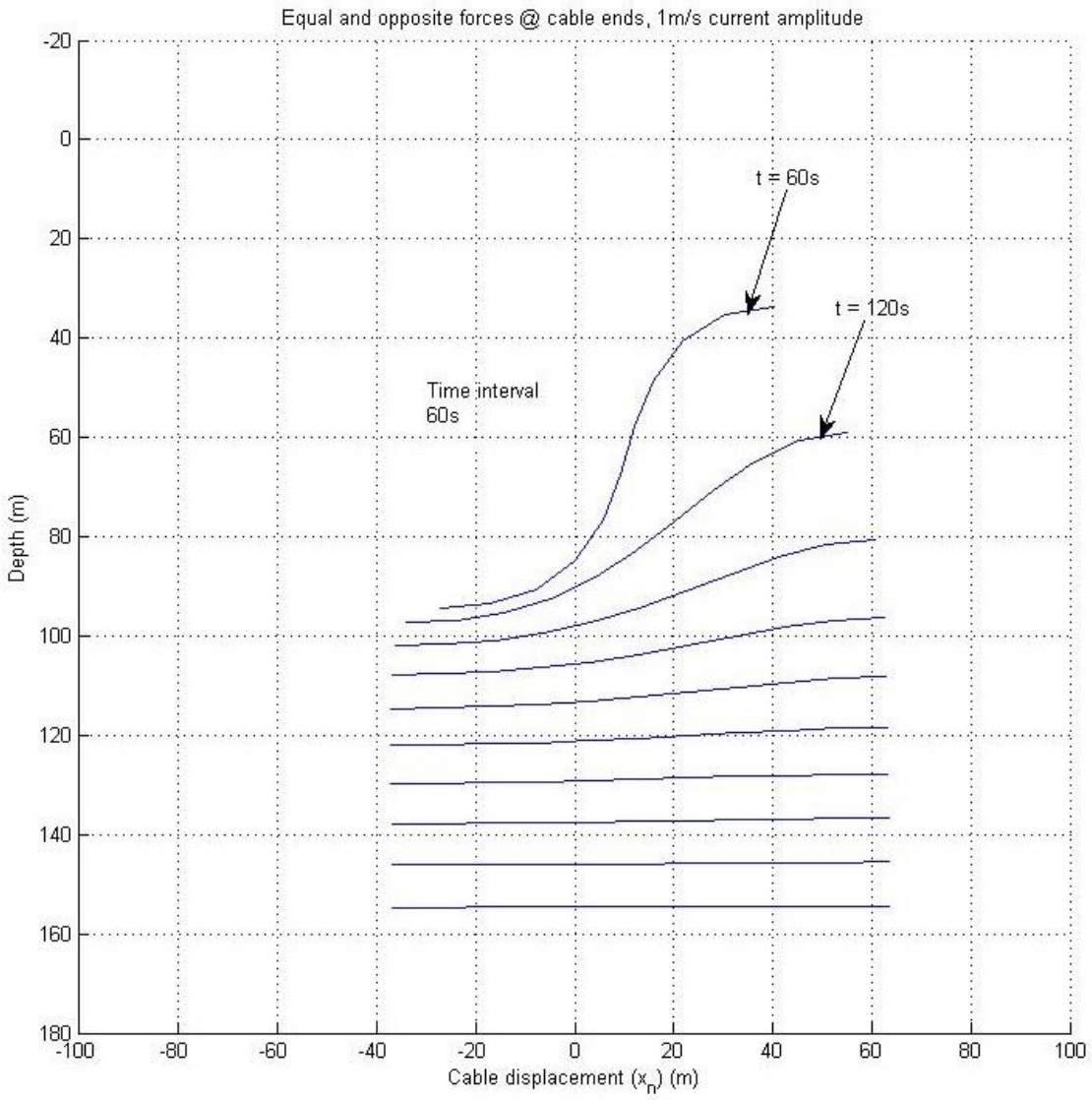

Figure 26. Equal and opposite forces at both ends, current amplitude 1m/s

For operating scenario 3, when equal and opposite forces are applied at both ends of the umbilical, it is expected to get a straight line shape parallel to the x-axis as the steady state configuration. This is indeed confirmed by viewing the results displayed on the above plots. Since there are no kinematic constraints at either of the cable ends, it keeps submerging, thus the varying depth of the whole configuration.

Chapter 5
Future directions

The purpose of this diploma thesis was to construct and validate a dynamic model that would describe the dynamic response of an umbilical tether in such a way, that it would be convenient for future control purposes from a mathematical perspective. This research was a success. Thus, future directions include the study the structural properties of the nonlinear scheme, namely controllability and observability. If first task is burdensome, then linearize the model about equilibrium points and try to study the structural properties of the resulting linearized model. It would be beneficial to do so, as the performance of the cable could be monitored by using position and velocity sensors. Implementation of control algorithms would allow it to achieve desired states, depending on the operating scenario and he task at hand.

Bibliography

1. Buckham, 'Dynamics modelling of low tension tethers for submerged Remotely operated vehicles', University of Victoria, 1997
2. Buckham et al., 'Dynamics and control of a towed underwater vehicle system, part I: model development', Ocean Engineering Vol. 30, 2003
3. Buckham et al., 'Dynamics and control of a towed underwater vehicle system, part II: model validation and turn maneuver optimization', Ocean Engineering Vol. 30, 2003
4. Huang, 'Dynamics analysis of three dimensional marine cables', Ocean Engineering Vol. 21, 1994
5. Leonard and Nath, 'Comparison of finite element and lumped parameter methods for oceanic cables', Eng. struct. Vol. 3, 1981
6. Buckham, Driscoll, Nahon, 'Development of a finite element cable model for use in low-tension dynamics simulation', Journal of Applied Mechanics, Vol. 4, 2004
7. Sanders, 'A three dimensional dynamic analysis of a towed system, Ocean Engineering, Vol. 9, 1982
8. Walton and Polachek, 'Calculation of transient motion of submerged cables', 1960
9. Ablow and Schechter, 'Numerical simulation of undersea cable dynamics', Ocean Engineering, Vol. 10, 1983
10. Milinazzo et al., 'An efficient algorithm for simulating the dynamics of towed cable systems', Ocean Engineering Vol. 14, 1987
11. Howell, 'Investigation of the Dynamics of low-tension cables', Massachusetts Institute of Technology, 1992
12. Gobat, 'Dynamics of geometrically compliant mooring systems', Unievrsity of California, San Diego, 1993
13. Gobat and Grosenbaugh, 'Application of the generalized α method to the time integration of the cable dynamics equations', Comput. Methods Appl. Mech. Engineering, 2001
14. Zhu, 'Nodal position finite element method and its application to dynamics of cable systems', Proceedings of I.M.E.C.E, 2008
15. Sun et al., 'Dynamic modelling of cable towed body using nodal position finite element method', Ocean Engineering Vol. 38, 2011
16. Vaz and Patel, 'Three dimensional behavior of elastic marine cabled in sheared currents', Applied Ocean Research Vol. 22, 2000
17. Vaz and Patel, 'Transient behavior of towed marine cables in two dimensions', Applied Ocean Reasearch Vol. 17, 1995
18. JJ Burgess, 'Equations of motion of a submerged cable with bending stiffness', 1992